Inelastic x-ray scattering studies of liquids and glasses

Giulio Monaco
ESRF, Grenoble (F)

outline:

- High-resolution IXS: what is it?
- Instrumentation: how do we do it?
- Data interpretation: what do we learn?
- Examples of studies of glasses
- Examples of studies of liquids

Scattering kinematics

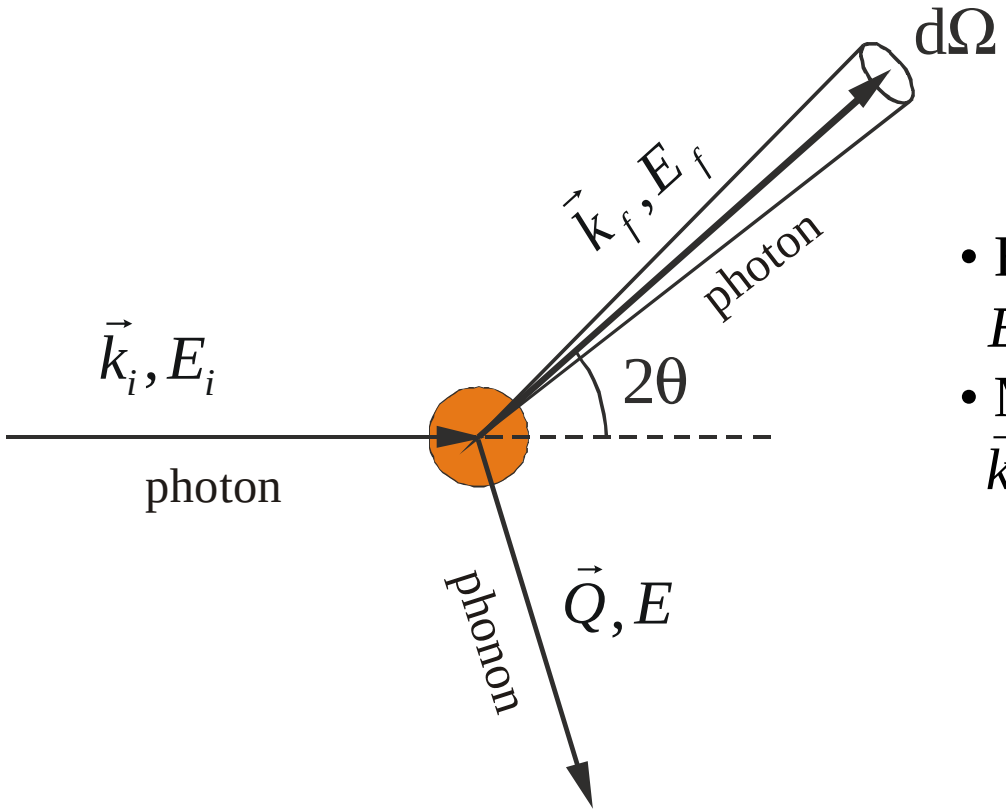

- Energy transfer:
  $E_f - E_i = E$ (1 – 500 meV)
- Momentum transfer:
  $\vec{k}_f - \vec{k}_i = \vec{Q}$ (1 – 100 nm^{-1})

$$\left|\vec{Q}\right| = 2\left|\vec{k}_i\right|\sin(\theta)$$

The momentum transfer is defined only by the scattering angle

Inelastic x-ray scattering

access to a rich excitation spectrum

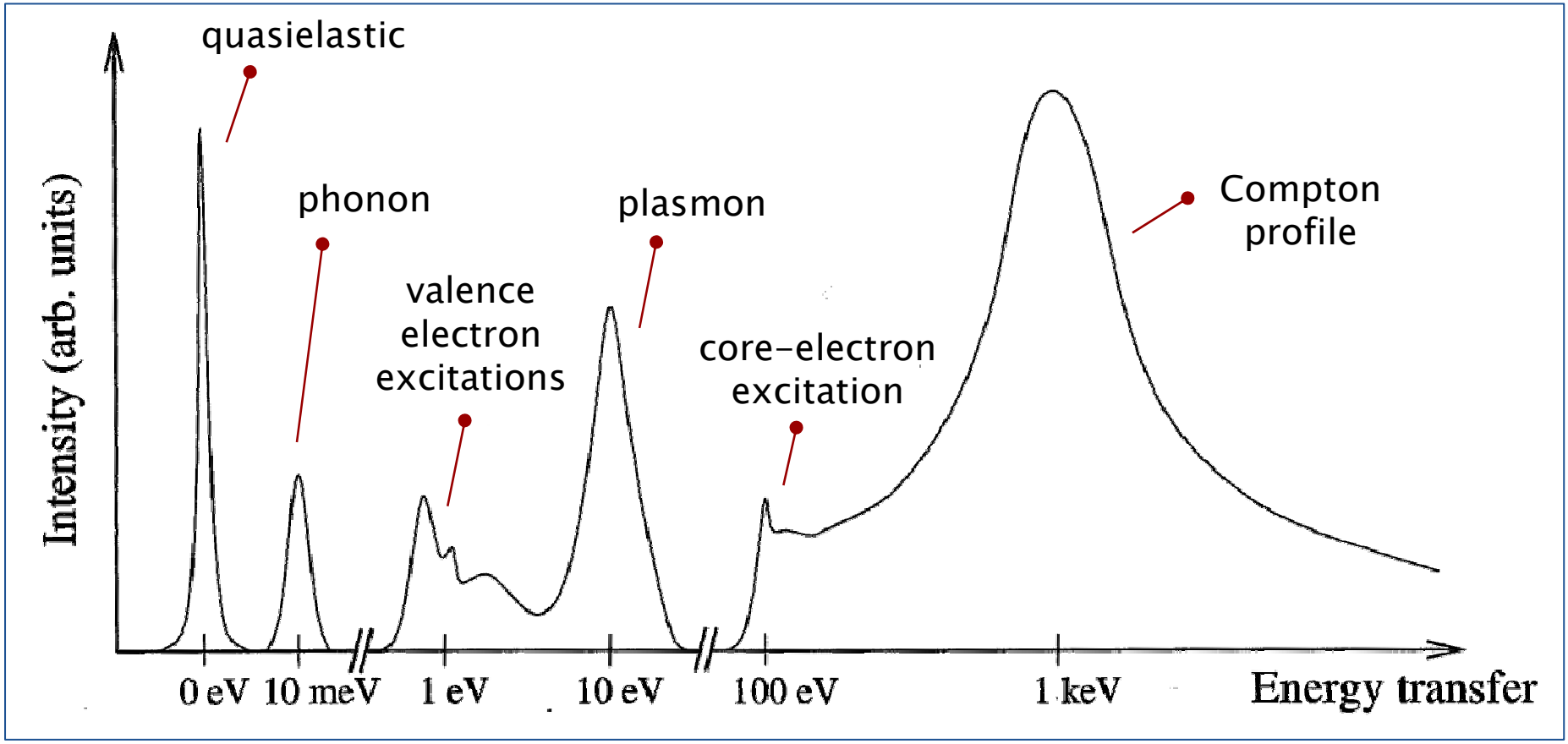

X-rays and phonon studies?

Two citations from standard text books

"When a crystal is irradiated with X-rays, the processes of photoelectric absorption and fluorescence are no doubt accompanied by absorption and emission of phonons. The energy changes involved are however so large compared with phonon energies that information about the phonon spectrum of the crystal cannot be obtained in this way."

W. Cochran in Dynamics of atoms in crystals, (1973)

"…In general the resolution of such minute photon frequency is so difficult that one can only measure the total scattered radiation of all frequencies, … As a result of these considerations x-ray scattering is a far less powerful probe of the phonon spectrum than neutron scattering. "

Ashcroft and Mermin in Solid State Physics, (1975)

Vibrational spectroscopy: historical insight

Infrared absorption - 1881
W. Abney and E. Festing, R. Phil. Trans. Roy. Soc. 172, 887 (1881)

Brillouin light scattering - 1922
L. Brillouin, Ann. Phys. (Paris) 17, 88 (1922)

Raman scattering – 1928
C. V. Raman and K. S. Krishnan, Nature 121, 501 (1928)

TDS: Phonon dispersion in Al – 1948
P. Olmer, Acta Cryst. 1 (1948) 57

INS: Phonon dispersion in Al – 1955
B.N. Brockhouse and A.T. Stewart, Phys. Rev. 100, 756 (1955)

IXS: Phonon dispersion in Be – 1987
B. Dorner, E. Burkel, Th. Illini and J. Peisl, Z. Phys. B – Cond. Matt. 69, 179 (1987)

NIS: Phonon DOS in Fe – 1995
M. Seto, Y. Yoda, S. Kikuta, X.W. Zhang and M. Ando, Phys. Rev. Lett. 74, 3828 (1995)

Inelastic Scattering from phonons

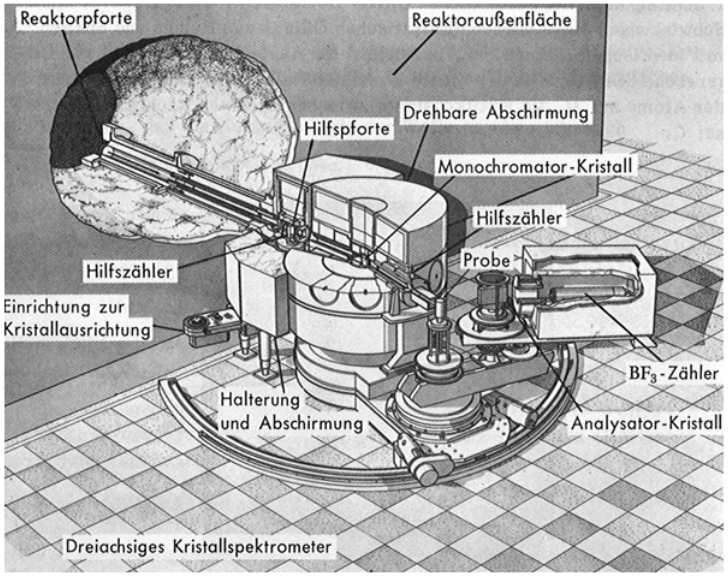

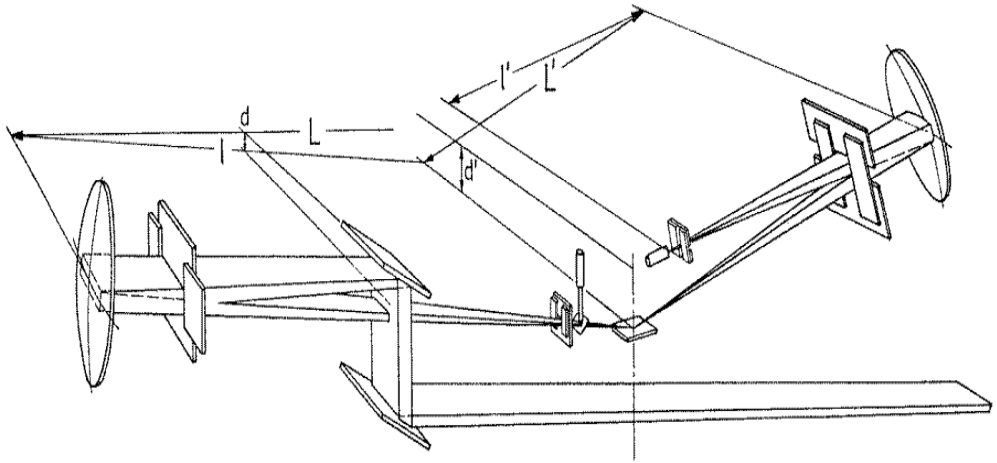

The instrument INELAX at the HARWI wiggler line of HASYLAB.

Brockhouse (1955)

Thermal neutrons:

E_i = 25 meV

k_i = 38.5 nm^{-1}

$\Delta E/E$ = 0.01 – 0.1

Burkel, Dorner and Peisl (1987)

Hard X-rays:

E_i = 18 keV

k_i = 91.2 nm^{-1}

$\Delta E/E \leq 1 \times 10^{-7}$

1987 – first IXS measurements

Z. Phys. B – Condensed Matter 69, 179–183 (1987)

Condensed Matter
Zeitschrift für Physik B
© Springer-Verlag 1987

First Measurement of a Phonon Dispersion Curve by Inelastic X-ray Scattering

B. Dorner *, E. Burkel, Th. Illini, and J. Peisl
Sektion Physik der Ludwig Maximilians Universität, München, Federal Republic of Germany

Received July 6, 1987

Inelastic scattering of 13.8 keV X-rays with very high energy resolution of $\Delta E = 55$ meV was used to measure the phonon dispersion curves for the *LA* and *LO* modes in the [00ξ] direction in Be. The results agree with inelastic neutron scattering data known from the literature. The X-ray scattering intensities of the phonon excitations for different momentum transfers are in very good agreement with the prediction from the scattering law.

HASYLAB

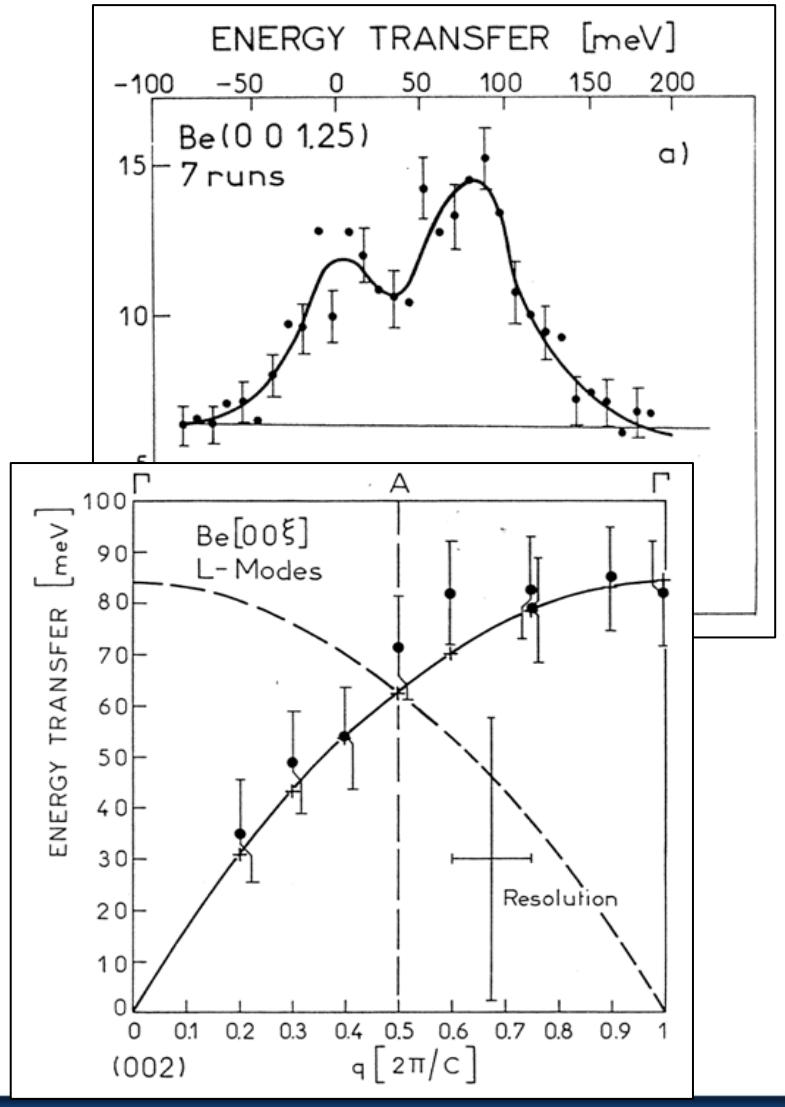

Inelastic x-ray scattering cross section

Electron-photon interaction Hamiltonian

$$H_{X-Th} = \frac{1}{2} r_0 \sum_j A^2\left(r_j, t\right)$$

Double-differential cross section

$$\frac{\partial^2 \sigma}{\partial \Omega \partial E} = r_0^2 \left(\vec{\varepsilon}_1 \cdot \vec{\varepsilon}_2\right)^2 \frac{k_1}{k_2} \sum_{I,F} P_I \left| \left\langle F \left| \sum_j e^{i\vec{Q}\vec{r}_j} \right| I \right\rangle \right|^2 \delta\left(E - E_f - E_i\right)$$

Thomson scattering cross section

The central approximation

Adiabatic approximation:

$$|I\rangle = |I_e\rangle|I_n\rangle \qquad |F\rangle = |I_e\rangle|F_n\rangle$$

for a mono-atomic system:

$$\frac{\partial^2\sigma}{\partial\Omega\partial E} = r_0^2\,(\vec{\varepsilon}_1\cdot\vec{\varepsilon}_2)^2\,\frac{k_1}{k_2}\,|f(Q)|^2\,S(\vec{Q},E)$$

Thomson scattering cross section

Atomic form factor

Dynamic structure factor

Dynamic structure factor

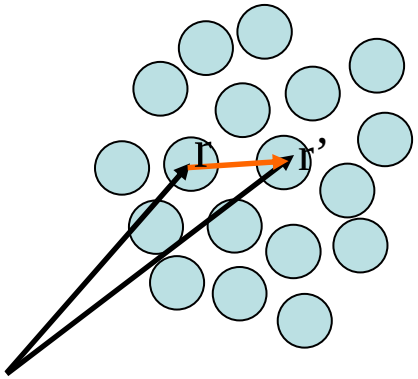

Dynamic structure factor S(**q**,ω):

space and **time** Fourier transform of G(|**r-r'**|,t)

$$S(q,\omega) = \int_{-\infty}^{\infty} dt\ e^{-i\omega t} \int_{-\infty}^{\infty} d^3r\ e^{-i\mathbf{k}\cdot\mathbf{r}} G(|\mathbf{r}-\mathbf{r}'|,t)$$

Pair correlation function G(|**r-r'**|,t):

G(|**r-r'**|,t) is the probability to find one particle at position **r** @ t=0 and a second particle at position **r'** @ time t

$$G(|\mathbf{r}-\mathbf{r}'|,t) = \langle \delta\rho(\mathbf{r}',0)\delta\rho(\mathbf{r},t)\rangle$$

Phonon spectroscopy

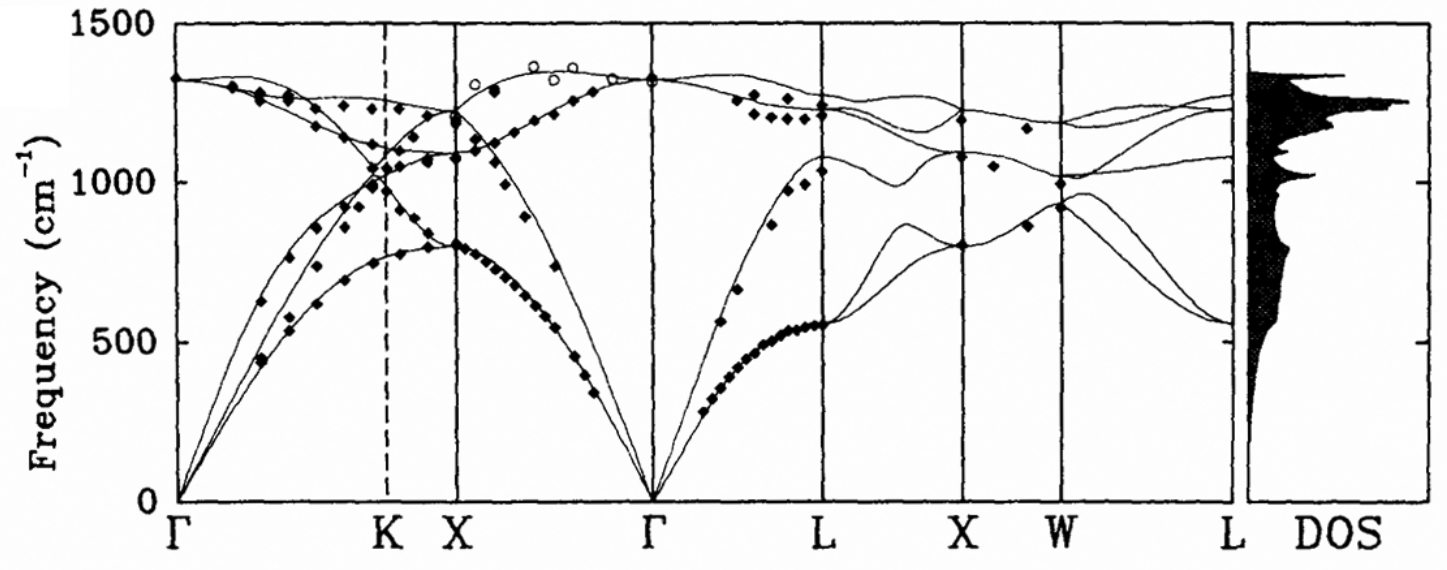

- Sound velocities
- Elasticity
- Interatomic force constants (potential)
- Dynamical instabilities (phonon softening)
- Anharmonicity
- Phonon-electron coupling

- Thermodynamics (C_V, S_V, θ_D, …)

IXS

$$\frac{\partial^2\sigma}{\partial E\partial\Omega} = r_0^2 \frac{k_1}{k_2}(\vec{\varepsilon}_1 \cdot \vec{\varepsilon}_2) f(Q)^2 \, S(\vec{Q}, E)$$

- no correlation between momentum- and energy transfer
- $\Delta E/E = 10^{-7}$ to 10^{-8}
- Cross section ~ Z^2 (for small Q)
- Cross section is dominated by photoelectric absorption (~ $\lambda^3 Z^4$)
- no incoherent scattering
- small beams: 100 μm or smaller

INS

$$\frac{\partial^2\sigma}{\partial E\partial\Omega} = b^2 \frac{k_1}{k_2} S(\vec{Q}, E)$$

- strong correlation between momentum- and energy transfer
- $\Delta E/E = 10^{-1}$ to 10^{-2}
- Cross section ~ b^2
- Weak absorption => multiple scattering
- incoherent scattering contributions
- large beams: typically several cm

Scientific themes

Disordered systems: explore new q-ΔE range

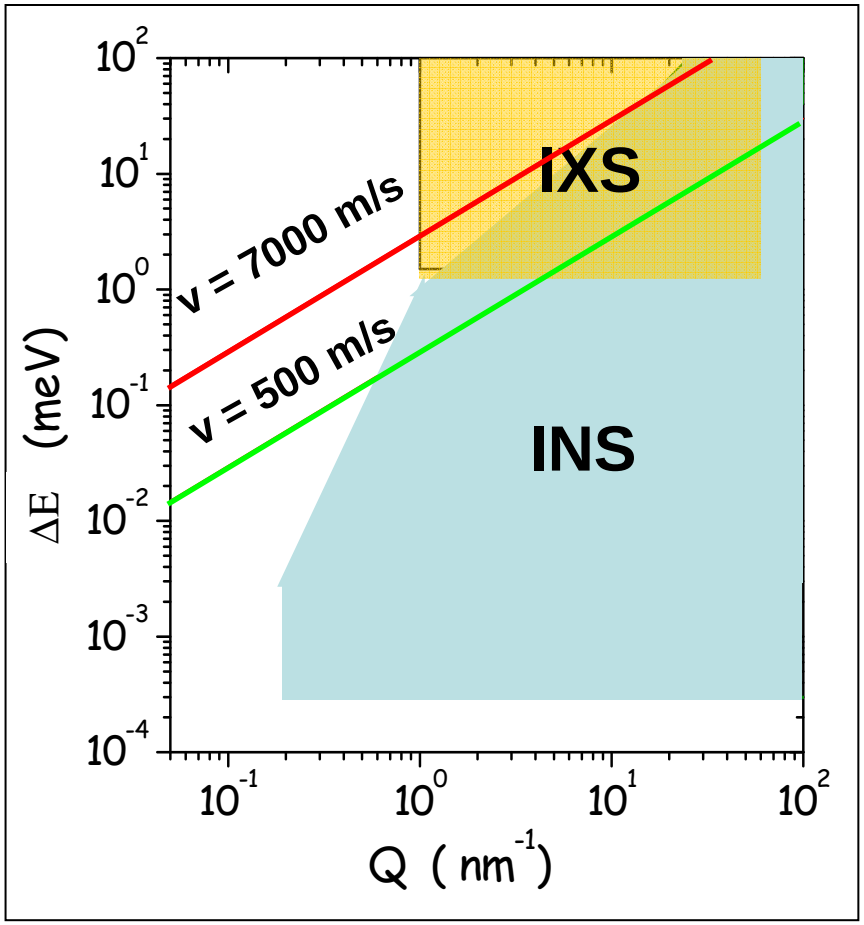

- Interplay between structure and dynamics
- Relaxations on the picosecond time scale
- Nature of sound propagation and attenuation

mesoscopic spatial range

Small sample volumes: 10^{-4} – 10^{-5} mm^3

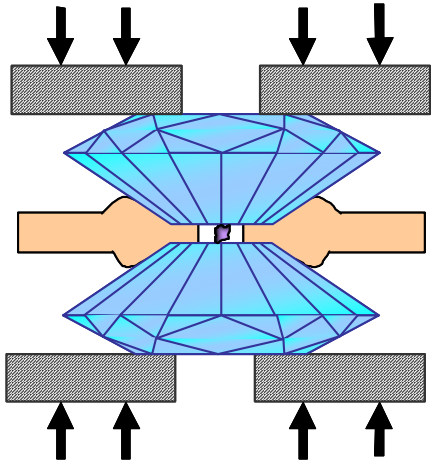

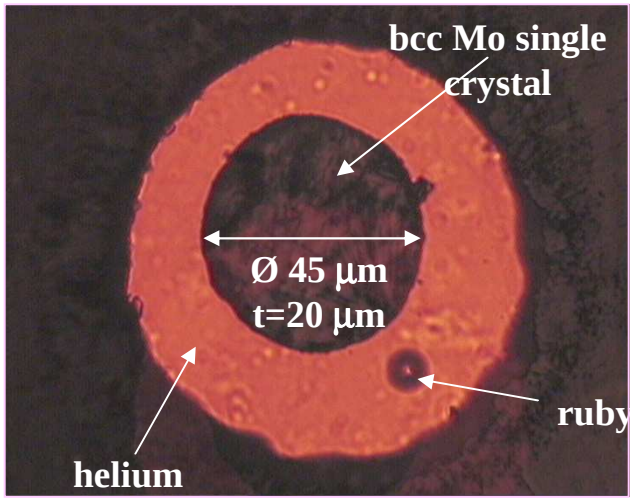

Diamond anvil cell

- **(New) materials in very small quantities**
- **Very high pressures > 1 Mbar**
- **Study of surface phenomena**

Inelastic x-ray scattering: instrumentation

ESRF: a European collaboration

The ESRF is financed by 19 countries.

How to do the experiment?

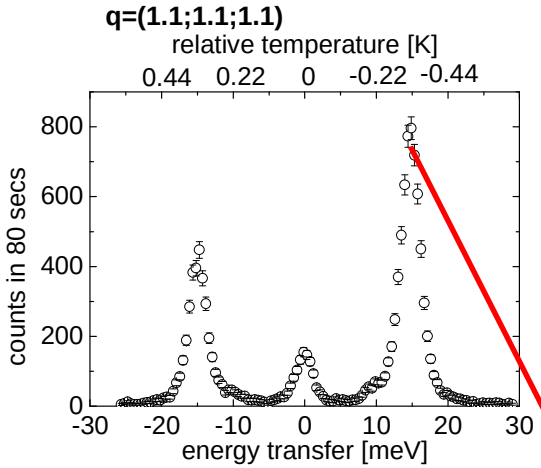

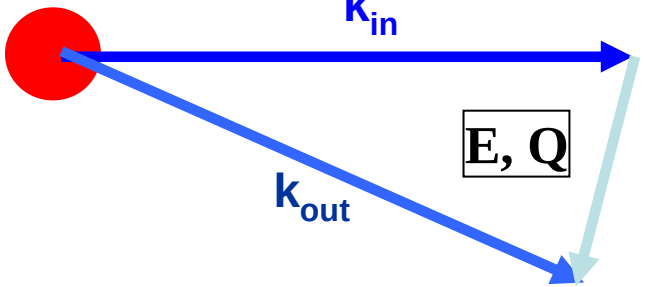

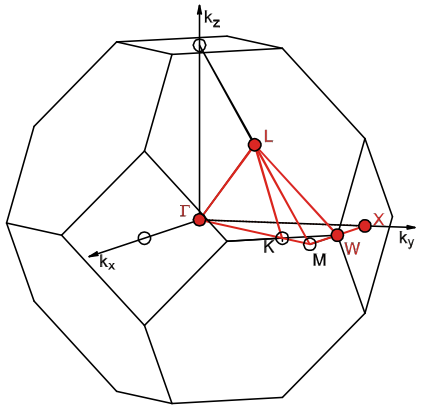

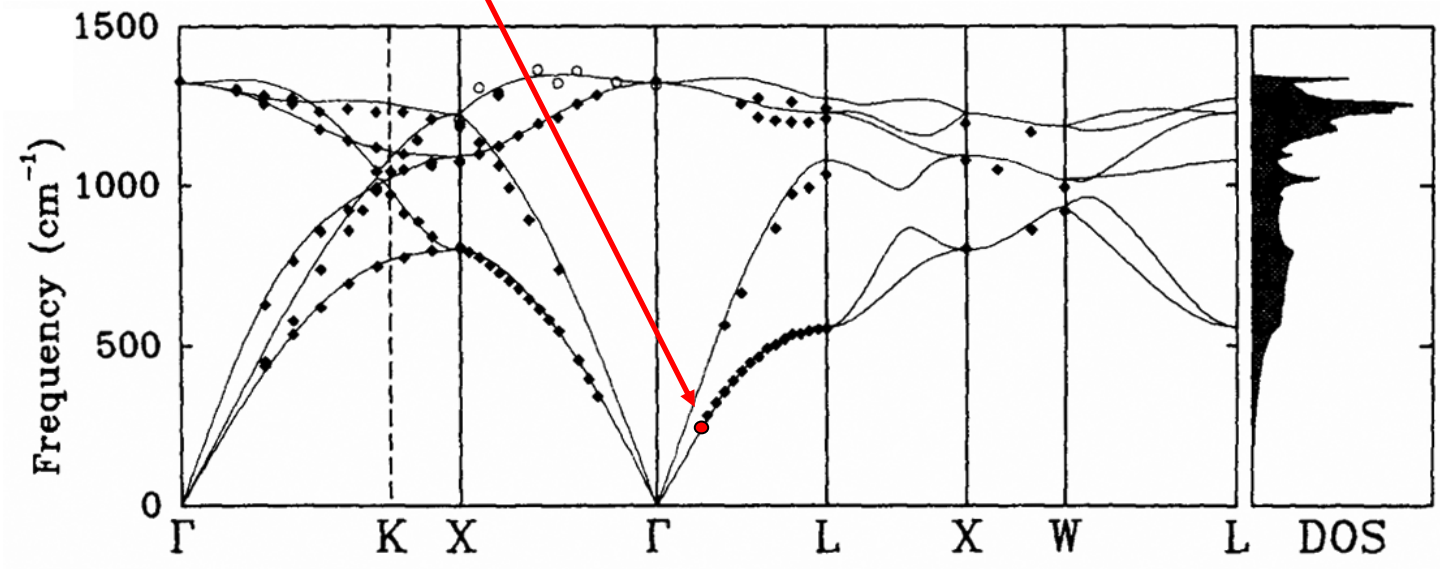

Experimental set-up

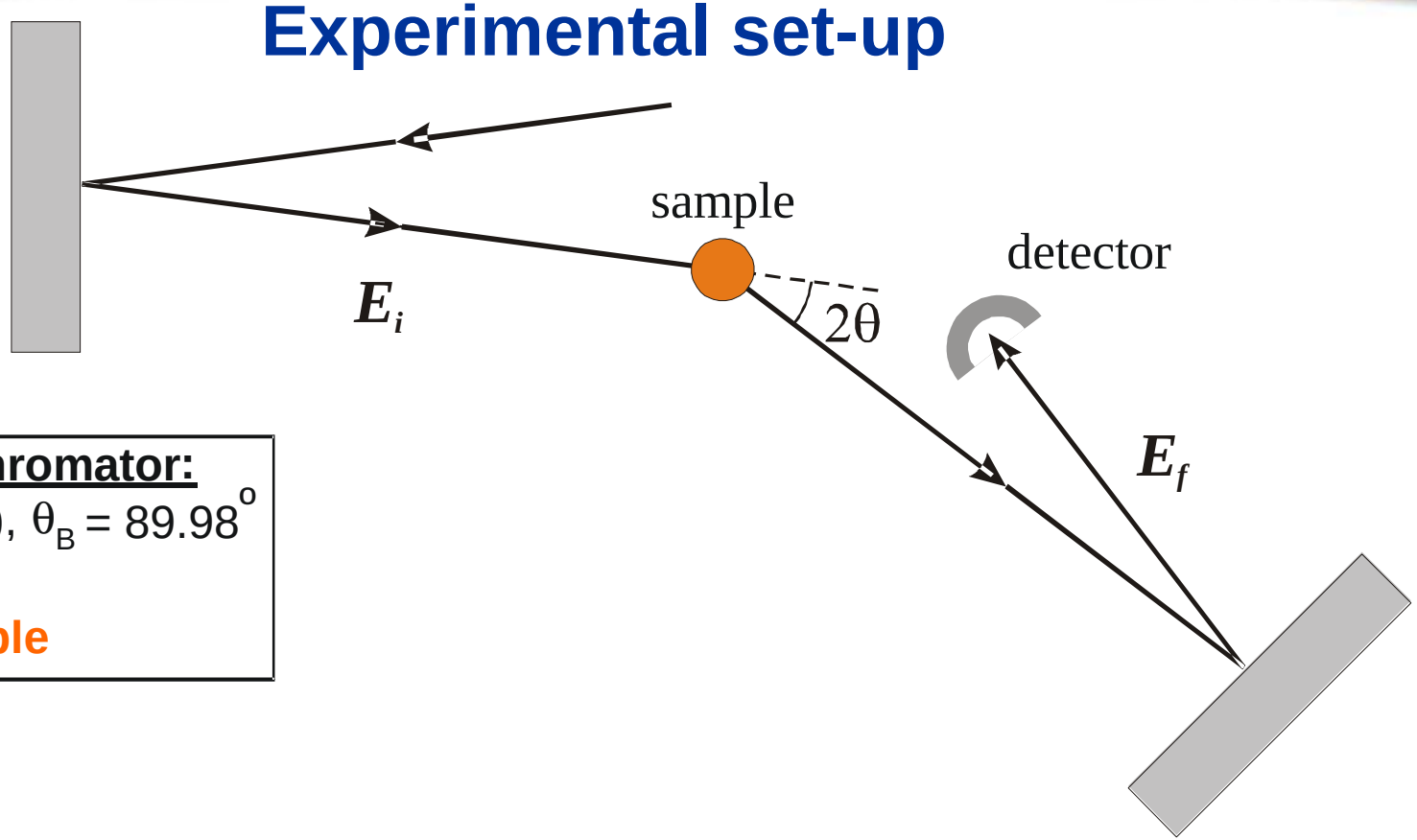

Monochromator:
Si(n,n,n), $\theta_B = 89.98^o$
n=7-13
λ_1 **tunable**

Spot size: 30 x 60 μm^2 (H x V)

Analyser:
Si(n,n,n), $\theta_B = 89.98^o$
n=7-13
λ_2 **constant**

meV-resolution inelastic x-ray scattering: the experiment

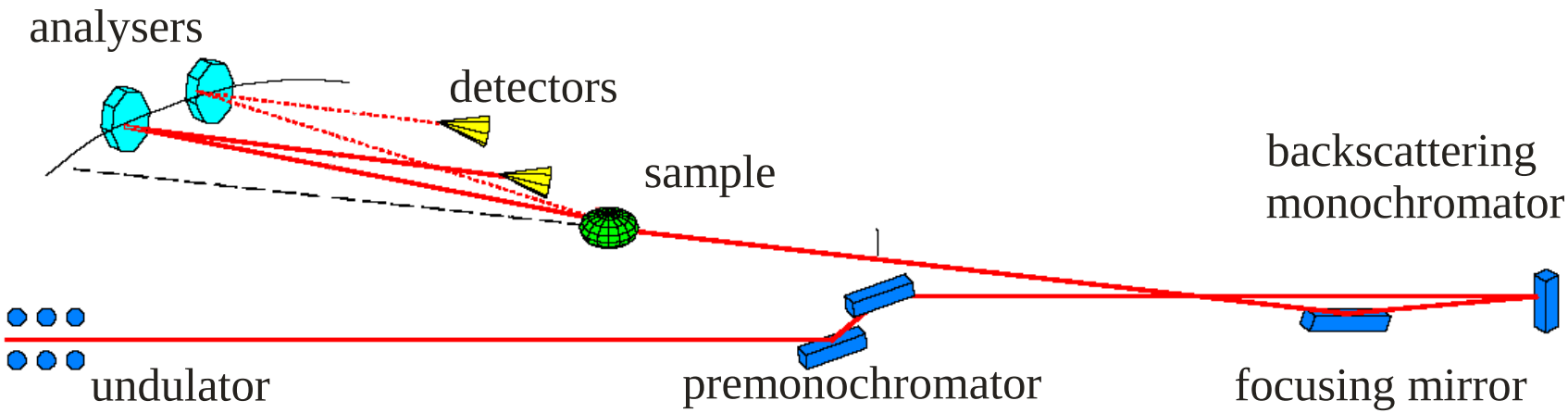

Energy scans are performed by main monochromator temperature change

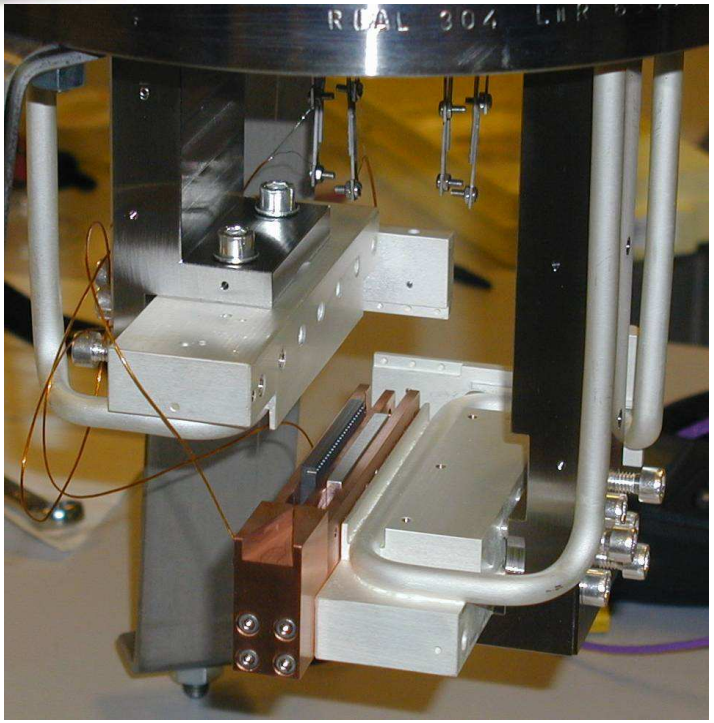

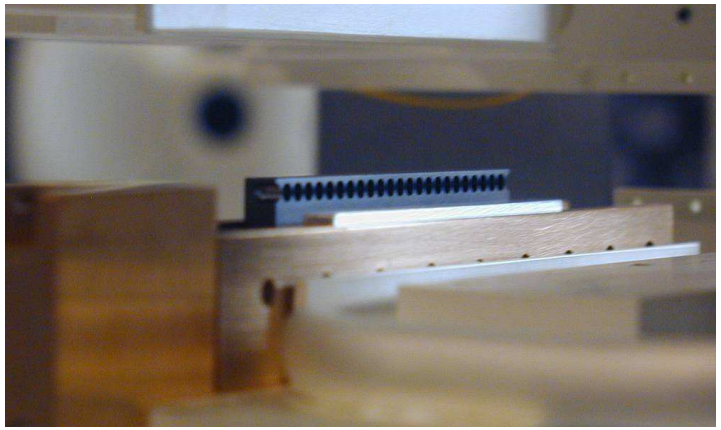

Collimating compound refractive beryllium lenses

Be compound refractive lenses installed 28.5 m far from the source. Their role is twofold:

- vertical collimation of the beam to better match the angular acceptance of the Si(111) premono;
- small footprint on the mirror

Si (n n n) reflection	# holes (R=1 mm)	Transmission	Residual divergence [µrad]	gain
8	13	0.96	2	1.02
9	16	0.92	2	1.06
11	24	0.92	2	1.20
13	34	0.90	2	1.30

Main monochromator

AIM:

- Reduce the bandwidth from ~10^{-4} to 10^{-7}-10^{-8}
- Accept the whole beam (V-divergence: ~15 μrad)

SOLUTION:

Backscattering crystal operating at high reflection order

Si(n n n) Reflection	E [eV]	ΔE [meV]	ΔE/E	3 x U35 flux [photons/s]
7	13839	5.3	$3.8 \cdot 10^{-7}$	$1.0 \cdot 10^{-11}$
8	15816	4.4	$2.8 \cdot 10^{-7}$	$7.6 \cdot 10^{-10}$
9	17793	2.2	$1.2 \cdot 10^{-7}$	$2.4 \cdot 10^{-10}$
11	21747	0.83	$4.7 \cdot 10^{-8}$	$4.6 \cdot 10^{-9}$
12	23724	0.73	$3.1 \cdot 10^{-8}$	$3.4 \cdot 10^{-9}$
13	25701	0.5	$1.9 \cdot 10^{-8}$	$1.0 \cdot 10^{-9}$

$\vartheta_B = 89.98°$, $\alpha = 85^o$

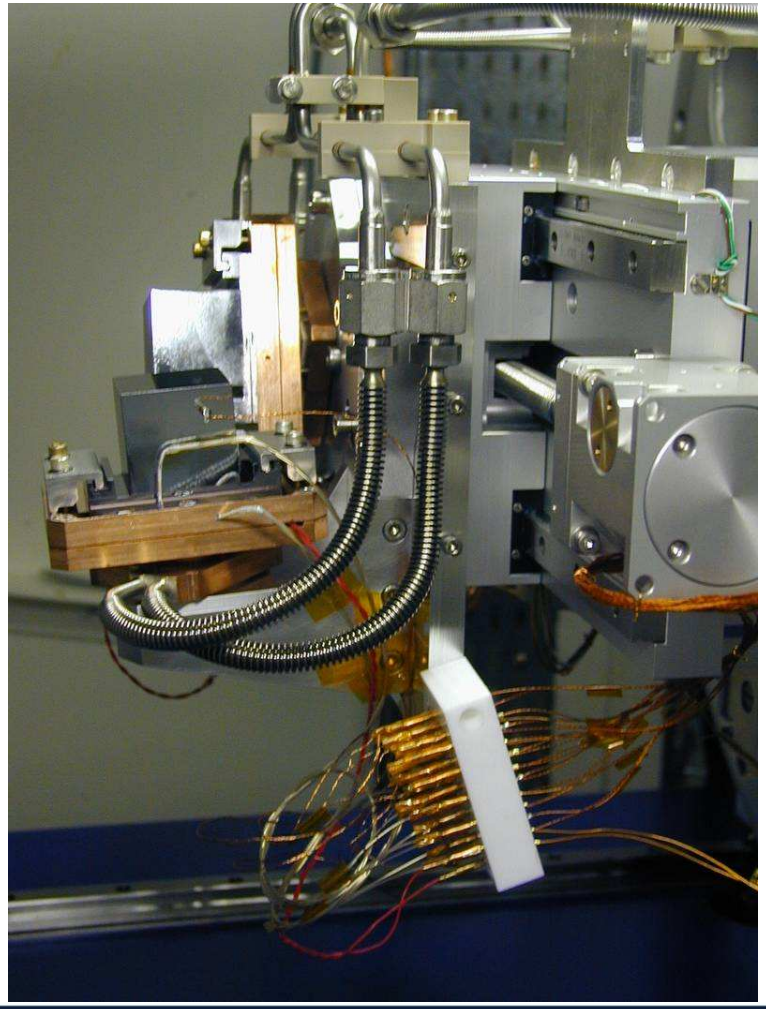

Heat load on the monochromator

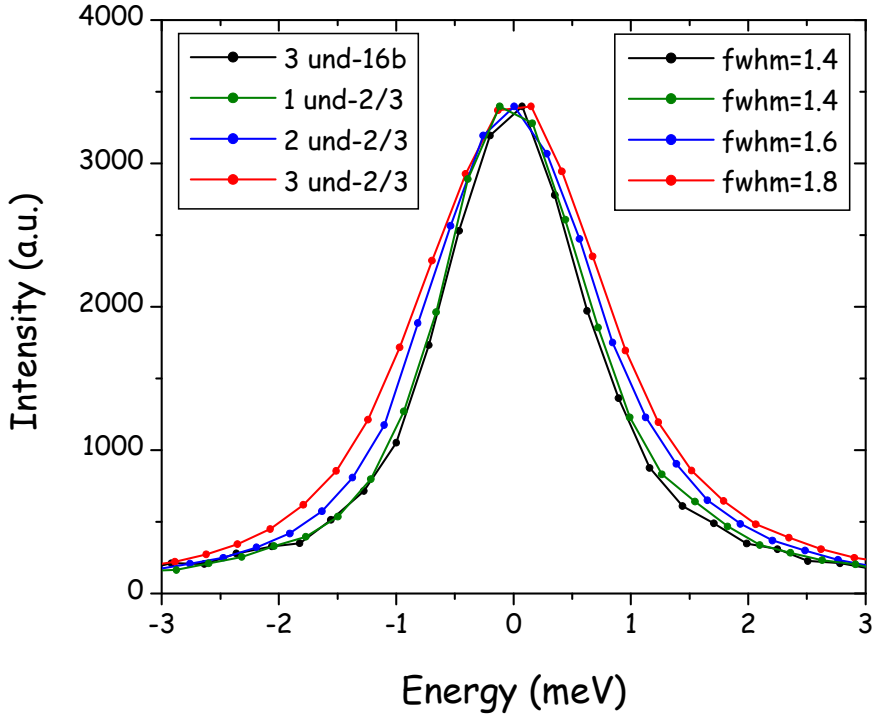

$$\Delta T_{ext} = P_d \, t \, k^{-1}$$

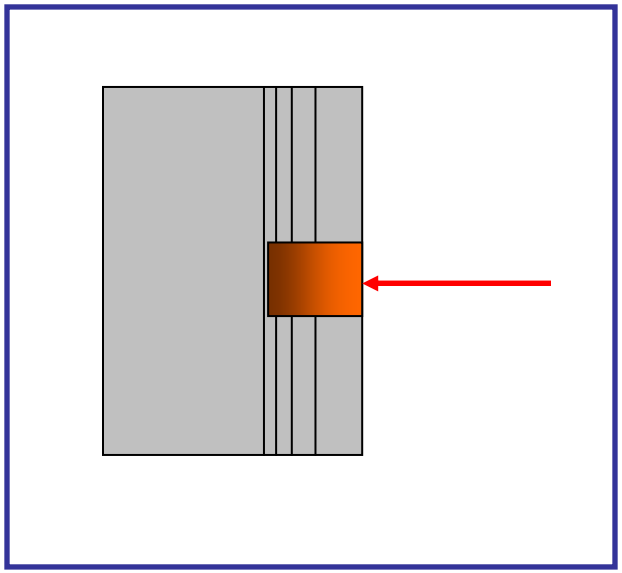

#u35	Φ	P	ΔT_{ext}	ΔE_{HL}	ΔE_{TOT}
	[photons/s]	[mW]	[mK]	[meV]	[meV]
1	$1.3 \cdot 10^{13}$	45	15	0.6	1.5
2	$2.6 \cdot 10^{13}$	90	31	1.2	1.8
3	$3.9 \cdot 10^{13}$	135	46	1.8	2.3

$$\Delta E_{HL} = 0.7 \cdot E \cdot \alpha \cdot \Delta T_{ext}$$

Cylindrical multilayer

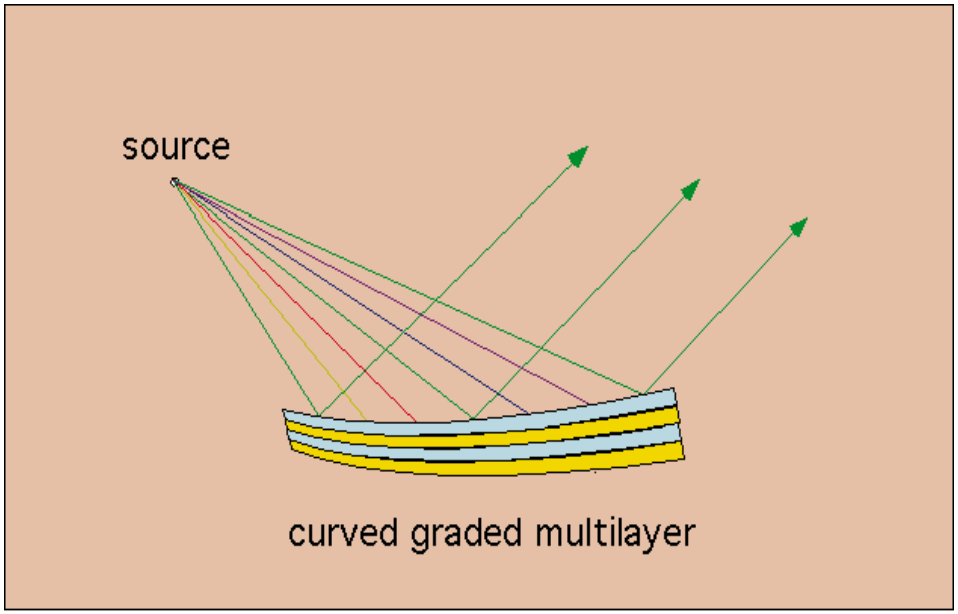

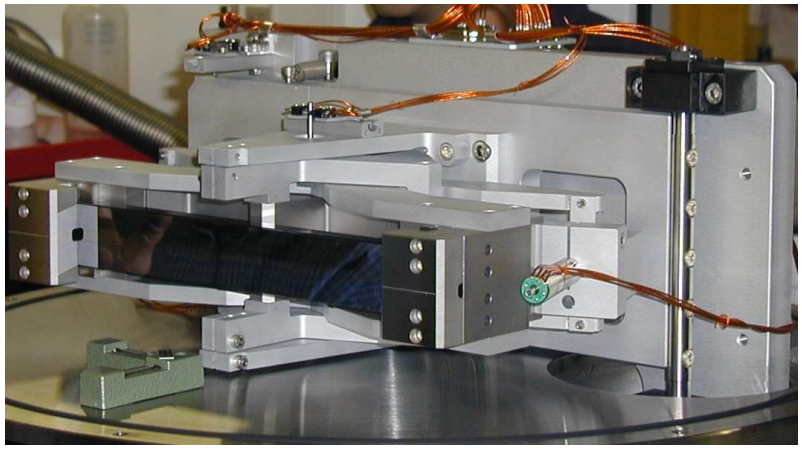

- materials: Ru/B_4C
- period: 3.0 nm at centre
- gradient: 6% lateral
- 24 cm footprint
- R= 336 m

p = 100 m
q = 2 m

disadvantages:
- large footprint
- sideways deflection

Horizontal focal spot: < 30 μm FWHM

High-resolution spectrometer

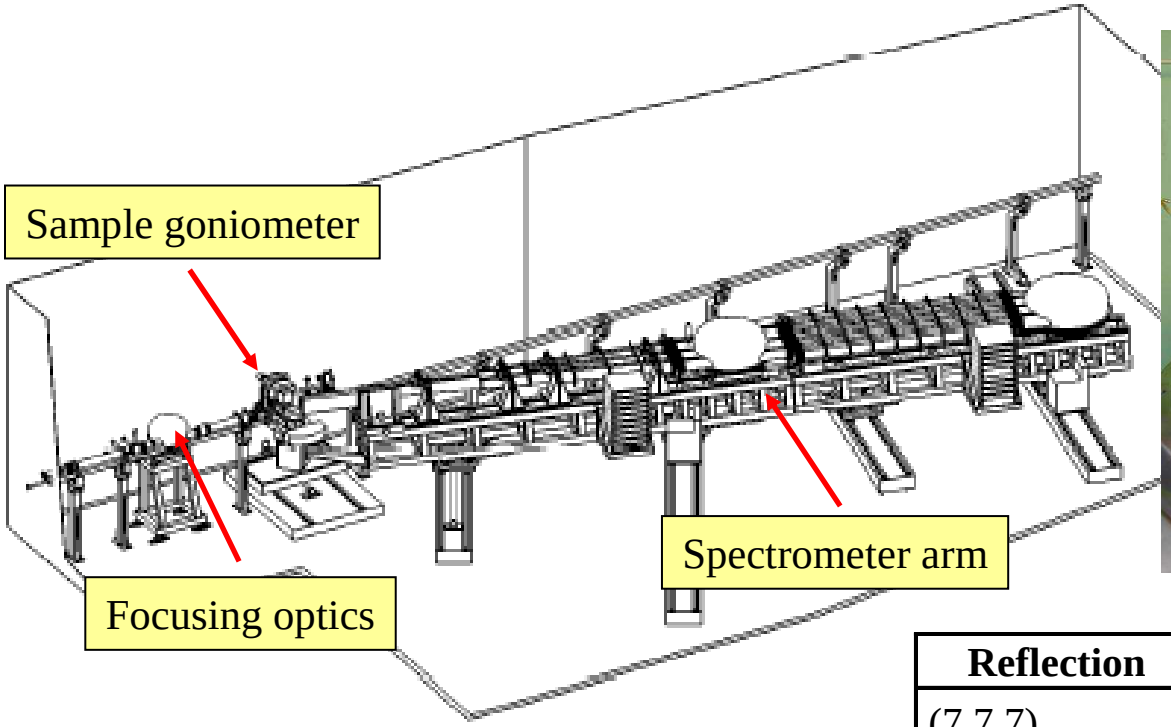

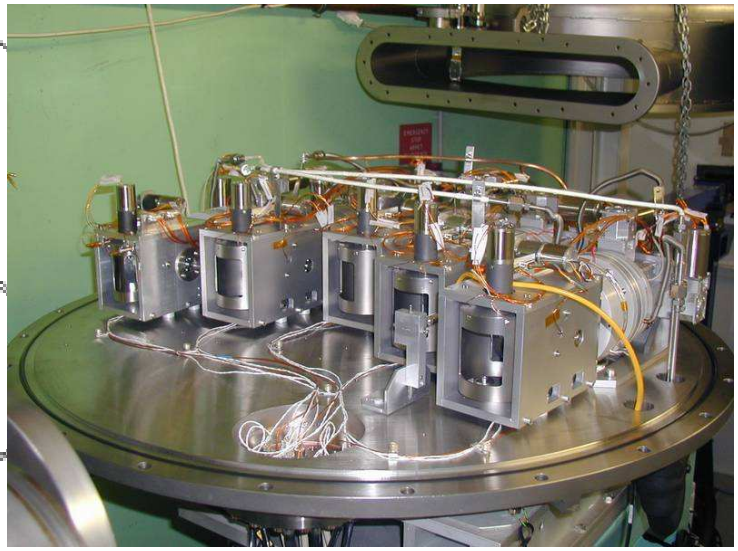

Reflection	ΔE [meV]	Q_{max} [nm^{-1}]
(7 7 7)	7	64
(8 8 8)	5.5	73
(9 9 9)	3.0	82
(11 11 11)	1.7	100
(13 13 13)	0.9	119

Spectrometer: analysers and detector

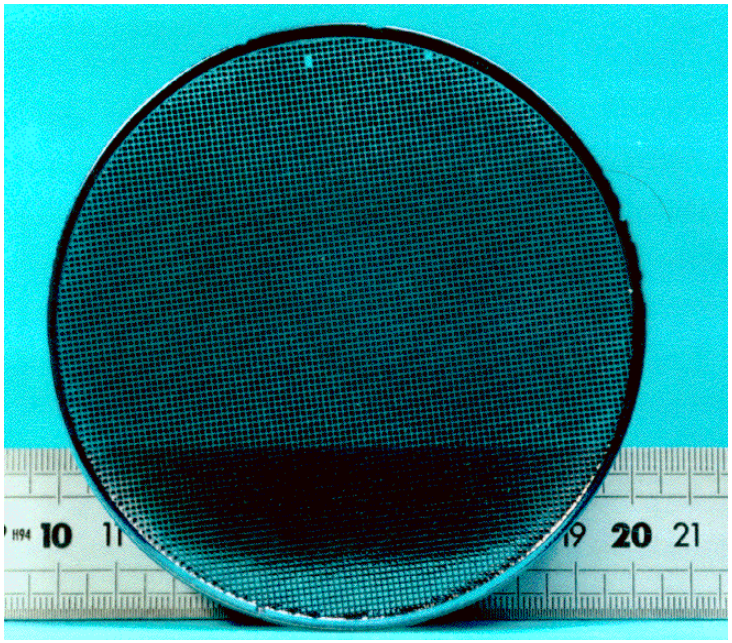

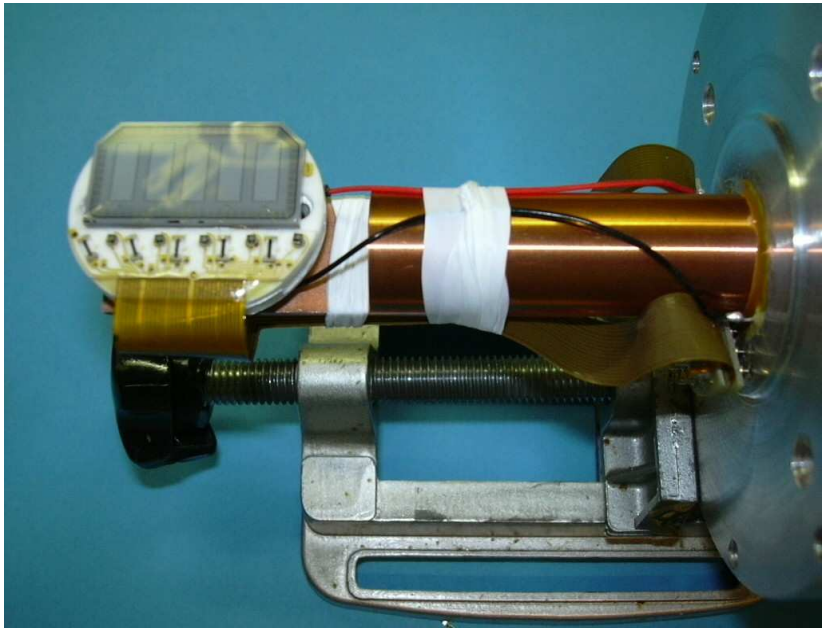

- ~10.000 cubes of 0.6x0.6x2.3 mm^3
- perfect crystal properties
- collection of sufficient solid angle

- 5 x 1.5 mm Si diodes at 20° incidence
- 1 count/20'
- Canberra – Eurisys
- Signal loss: 4% (15%) at n=11 (n=13)

IXS set-up: energy scan

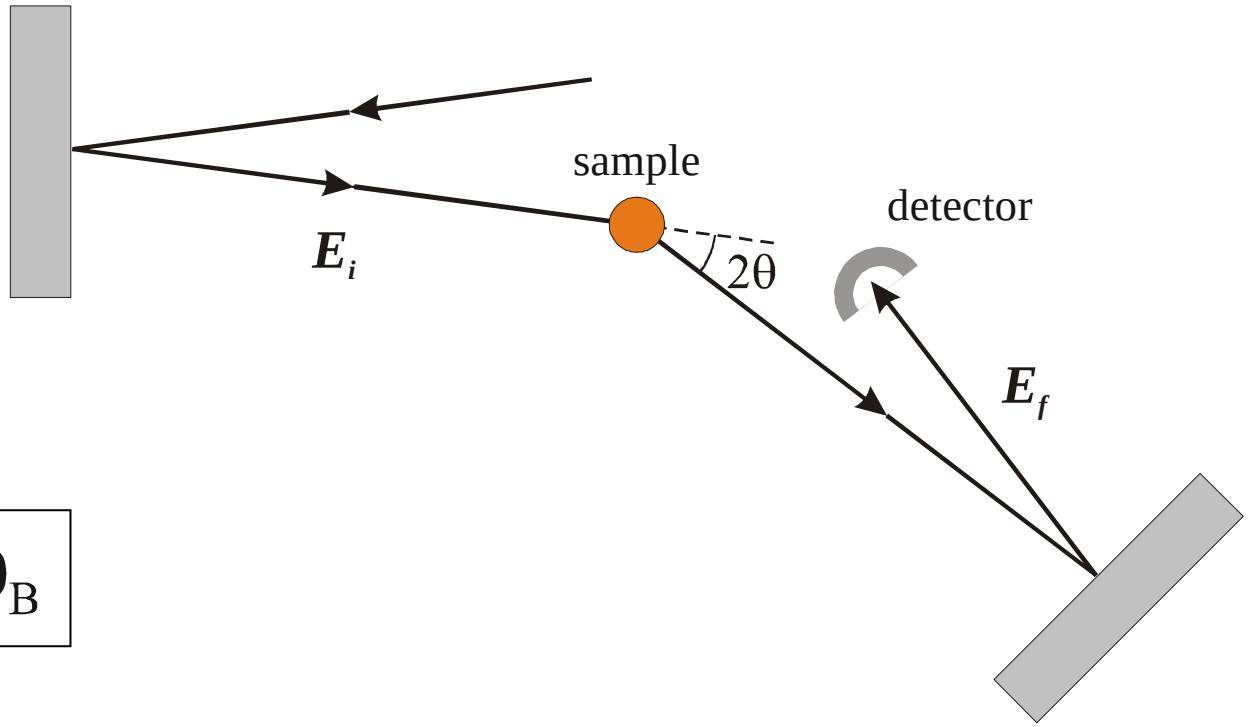

$$\mathbf{Q} = 4\pi/\lambda \cdot \sin(\theta)$$

$$\lambda = 2 \cdot d(T)\ \sin\theta_B$$

$$\Delta d/d = \Delta E/E = -\alpha(T) \cdot \Delta T \ (\alpha = 2.58 \cdot 10^{-6} \text{ at RT})$$

Reminder of Hydrodynamics & relaxation processes

Simple Hydrodynamics - I

Describes the long-lived, collective excitations
(tool to evaluate $S(q,\omega)$ in the low-q & low-ω regime

For a simple monatomic fluid:

- continuity equation (conservation of matter)
- force equation (conservation of momentum)
- heat-exchange equation (conservation of energy)

+ constitutive relations (response of the system to external constraints)

Assumptions:

- The fluid is a continuous medium, locally homogeneous and isotropic
- Three state variables related through the equation of state
- Local thermodynamic equilibrium
- Transport processes described by linear laws

Simple Hydrodynamics - II

Dynamic structure factor:

$$\frac{S(q,\omega)}{S(q)} = 2Re\lim_{\varepsilon\to 0}\frac{\left\langle \delta\rho_q^*(0)\delta\tilde{\rho}_q(s=\varepsilon+i\omega)\right\rangle}{\left\langle \delta\rho_q^*(0)\delta\rho_q(0)\right\rangle}$$

Simple hydrodynamics result:

$$\frac{S(q,\omega)}{S(q)} = \frac{\gamma-1}{\gamma}\frac{2\chi q^2}{\omega^2+(\chi q^2)^2} + \frac{1}{\gamma}\frac{2\Gamma q^2}{(\omega^2-c^2q^2)^2+(\omega\Gamma q^2)^2}$$

With $\Gamma = \frac{1}{2}[\nu_l + (\gamma-1)\chi]$

Info on: c, χ, γ, ν_l , χ_T

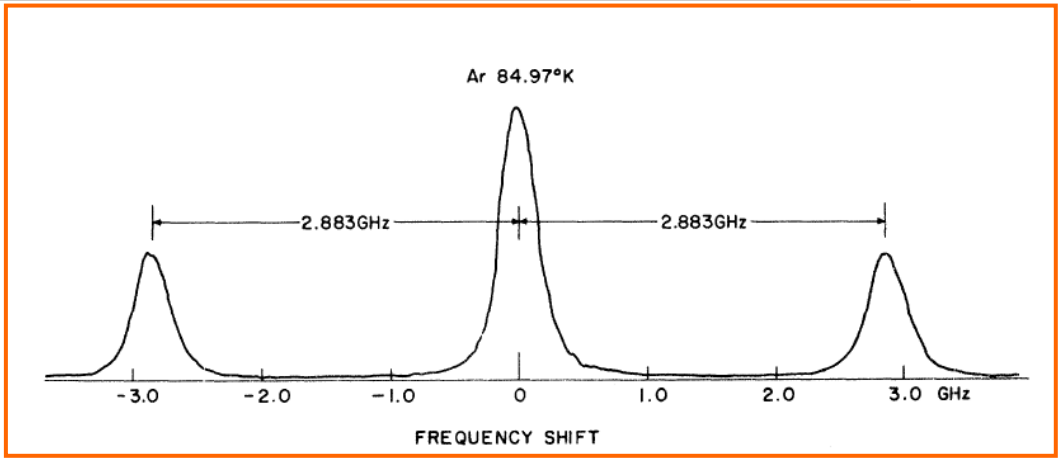

Fleury & Boon, Phys. Rev. 186, 244 (1969)

Relaxational dynamics in liquids

Well defined resonances (α–relaxation peaks) appear in susceptibility spectra. Their position strongly depends on T

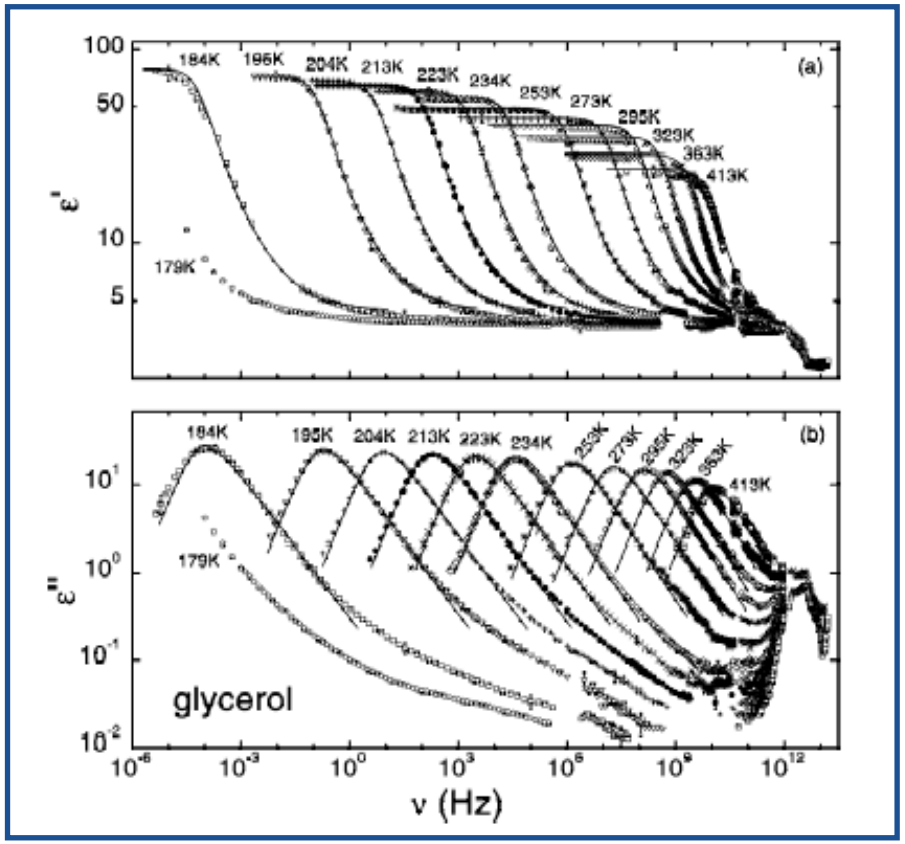

Lunkenheimer and Loidl, Chem. Phys. 284, 205 (2002)

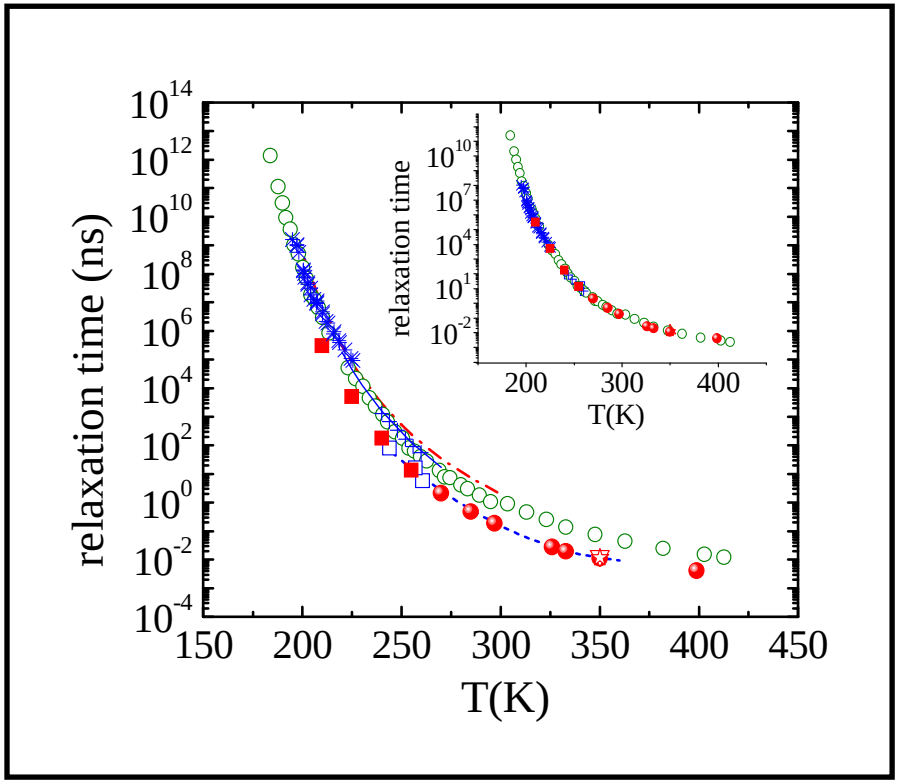

Comez et al., J. Chem. Phys. 119, 6032 (2003)

The α–relaxation scale appears to be universal. Its dependence on T closely follows that of the viscosity

Viscoelasticity

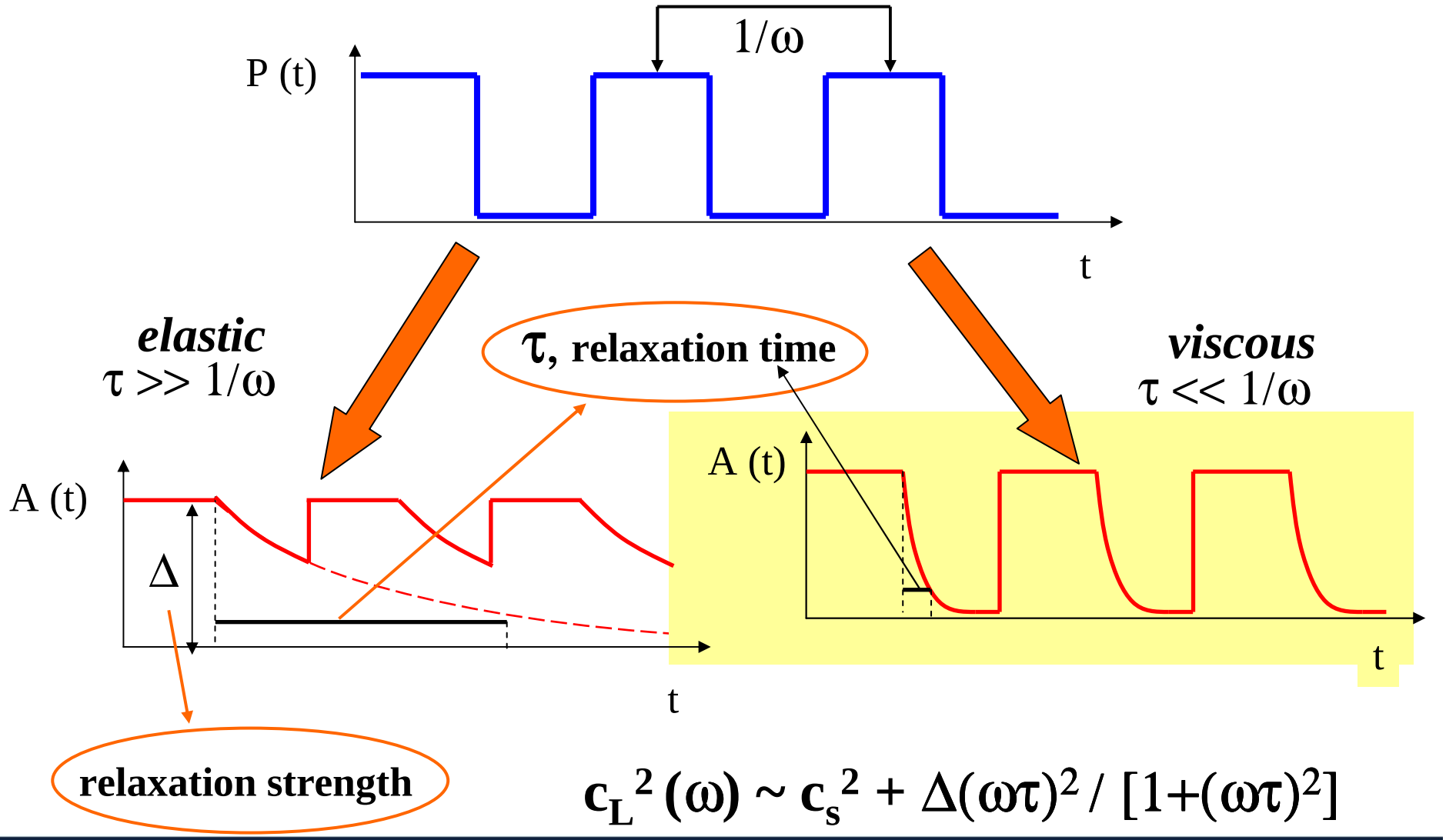

$$c_L^2(\omega) \sim c_s^2 + \Delta(\omega\tau)^2 / [1+(\omega\tau)^2]$$

The dynamic structure factor - 1

Generalized Langevin equation for $\phi_q(t)$

$$\ddot{\Phi}_q(t) + \omega_o^2(q)\ \Phi_q(t) + \int_o^t m_q(t-t')\ \dot{\Phi}_q(t')\ dt' = 0$$

Corresponding expression for the dynamic structure factor

$$S(q,\omega) = \frac{2\,S(q)\,\omega_o^2(q)}{\omega}\ \mathrm{Im}\left[\ \omega^2 - \omega_o^2(q) - i\omega m_q(\omega)\ \right]^{-1}$$

with

$$\omega_o^2(q) = \frac{(v_o q)^2}{S(q)}$$

(2nd sum rule)

Simple Hydrodynamics

$$m_q(t) = c_T^2\ q^2\ (\gamma - 1)\ e^{-D_T\ q^2\ t} + 2\nu_l\ q^2\ \delta(t)$$

The dynamic structure factor - 2

When the conditions $\omega \tau_m << 1$ and q a $<< 1$ no longer hold, the atomic dynamics is influenced both by structure and relaxational effects and we have to move from the Simple Hydrodynamics to the Generalized Hydrodynamic approach.

thermal diffusion term ⟶ $\omega_o^2(q)[\gamma(q)-1]\ e^{-D_T(q)q^2 t}$

viscosity relaxation term ⟶ $K_l(q,t)$

in particular:

$$\begin{cases} i)\ \chi_T \rightarrow S(q)/\rho_N K_B T \\ ii)\ q^2 \nu_l \rightarrow K_l(q,t) \end{cases}$$

and, as a connection with Simple Hydrodynamics:

$$\lim_{q\to 0} \int_0^\infty K_l(q,t)\ dt = q^2 \nu_l$$

Dispersion and absorption of the sound waves

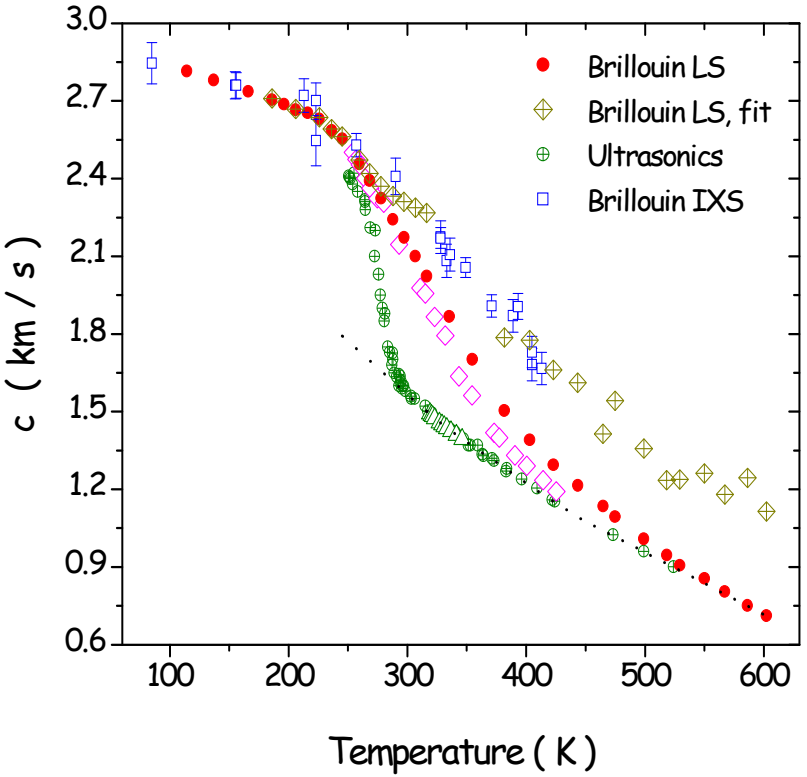

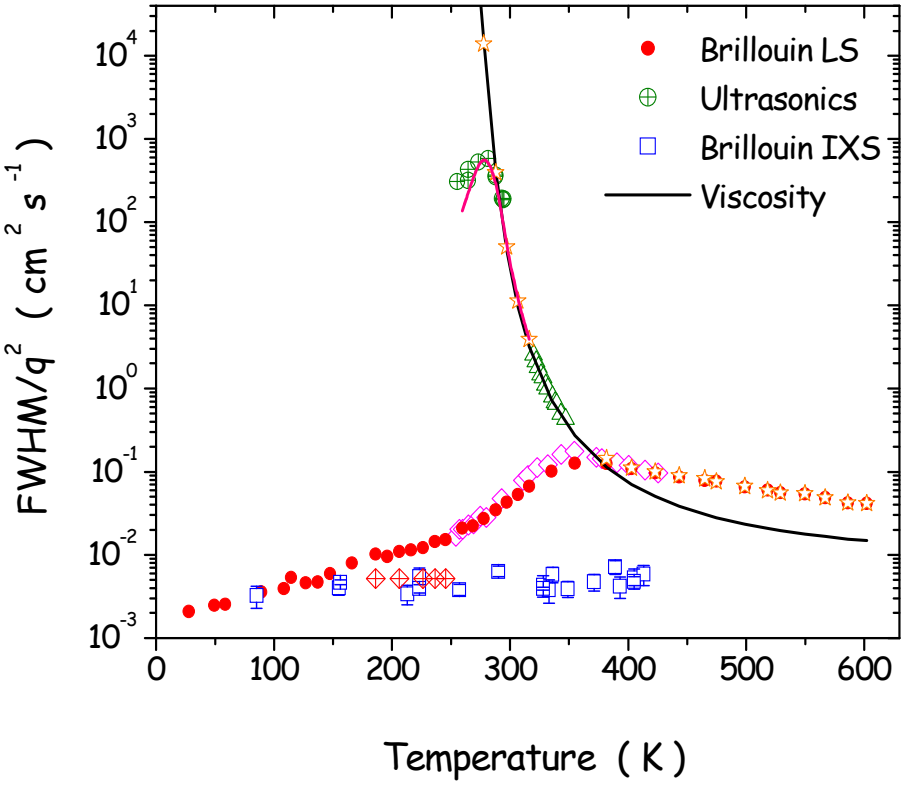

g.m. et al., Phys. Rev. E 63, 061502 (2001)

The density fluctuations spectrum

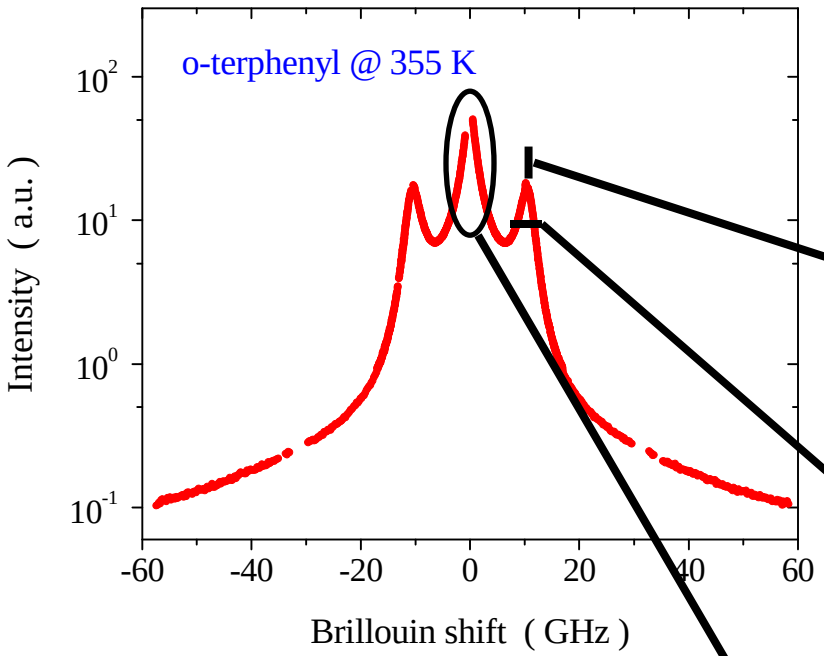

g.m. et al., Phys. Rev. E 63, 061502 (2001)

$$\frac{S(q,\omega)}{S(q)} = \frac{2}{\omega\,\chi_T(q)}\ \mathrm{Im}\left[\frac{\rho\,\omega^2}{q^2} - M_T(q,\omega)\right]^{-1}$$

$$\omega_{mc} = \sqrt{\frac{q^2\ M_T'(q,\omega_{mc})}{\rho}}$$

$$FWHM = \omega_{mc}\,\frac{M_T''(q,\omega_{mc})}{M_T'(q,\omega_{mc})} = 2\ \alpha\ c(\omega_{mc})$$

$$\frac{S(q,\omega)}{S(q)} \xrightarrow{\omega\to 0} \frac{2}{\omega\,\chi_T(q)}\ \mathrm{Im}\frac{1}{M_T(q,\omega)} = \frac{2\ \chi_T''(q,\omega)}{\omega\,\chi_T(q)}$$

Models for the memory function – DHO

(a) $\gamma \approx 1$

well verified in the study of glasses with IXS

(b) $\omega\ \tau_c\ (q) \gg 1$

$$m_q\ (t) = 2\ \gamma_0\ (q)\ \delta\ (t) + q^2\ \Delta^2\ (q)$$

with:

$f_q = 1 - c_o^2 / c_\infty^2\ (q)$

$$q^2\ \Delta^2 (q) = \omega_\infty^2\ (q) - \omega_0^2$$

$$\ddot{\Phi}_q(t) + \gamma_0\ (q)\ \dot{\Phi}_q(t) + \omega_o^2\ (q)\ \Phi_q(t) = q^2\ \Delta^2 (q)$$

$$\frac{S(q,\ \omega)}{S(q)} = f_q\ \delta\ (\omega) + (1 - f_q)\ \frac{2\ \omega_\infty^2\ (q)\ \gamma_0\ (q)}{\left[\omega^2 - \omega_\infty^2\ (q)\right]^2 + \left[\omega\ \gamma_0\ (q)\right]^2}$$

$c_\infty\ (q)$ limiting sound speed
$\gamma_o\ (q)$ q^2 times non-relaxing viscosity
f_q non ergodicity factor

FIT PARAMETERS

Examples of experiments on glasses

The universal anomalies of glasses

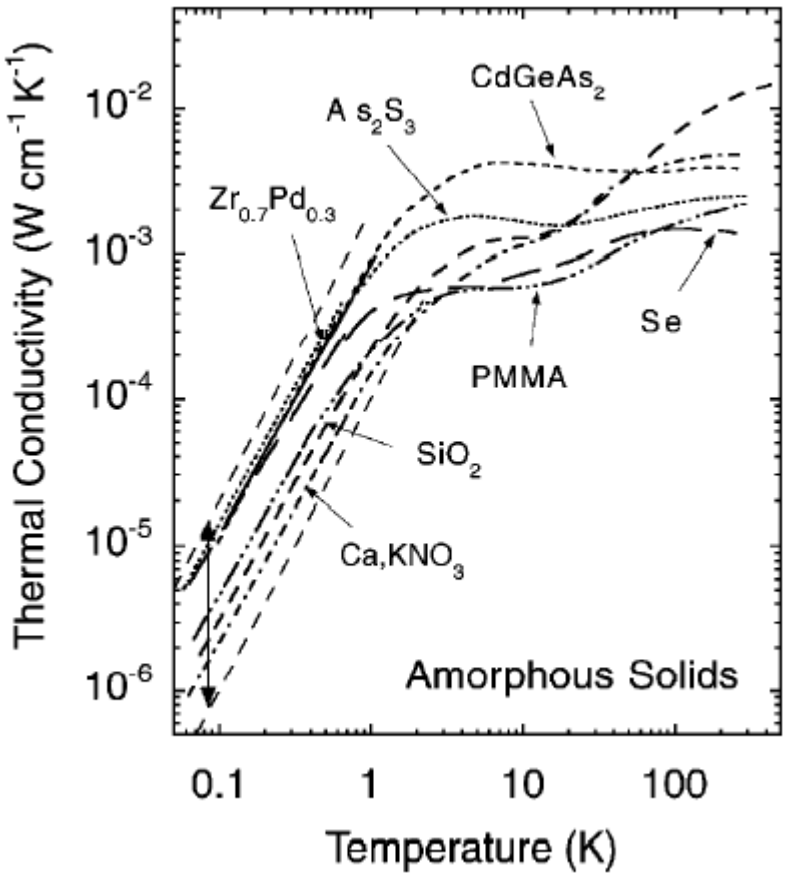

Pohl et al., Rev. Mod. Phys. 74, 991 (02)

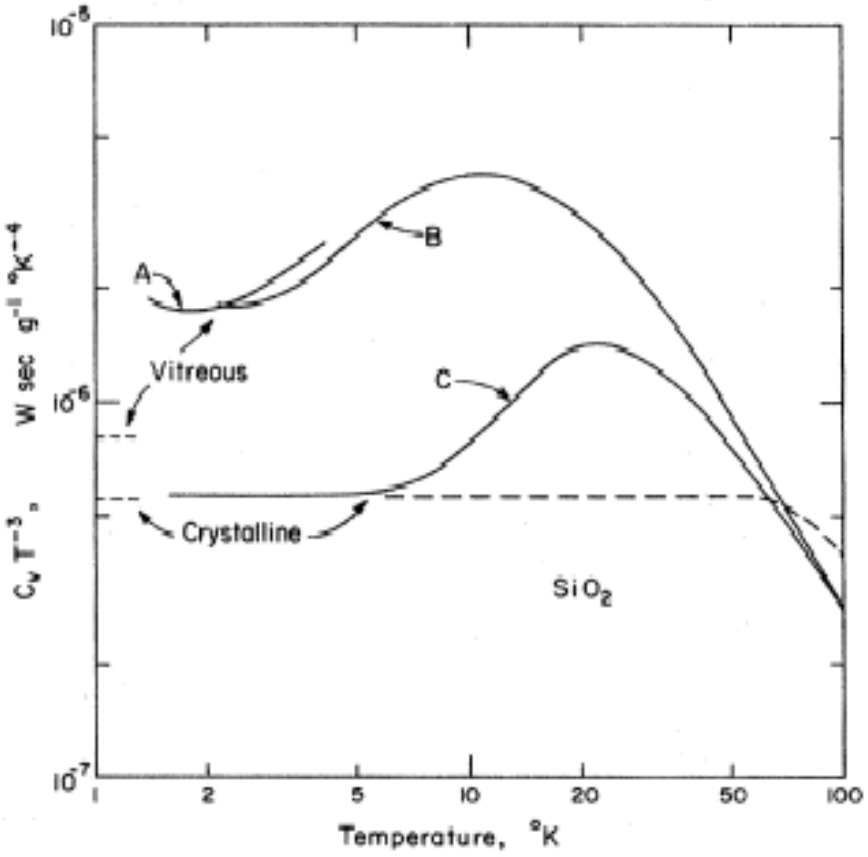

Zeller and Pohl, PRB 4, 2029 (71)

The boson peak

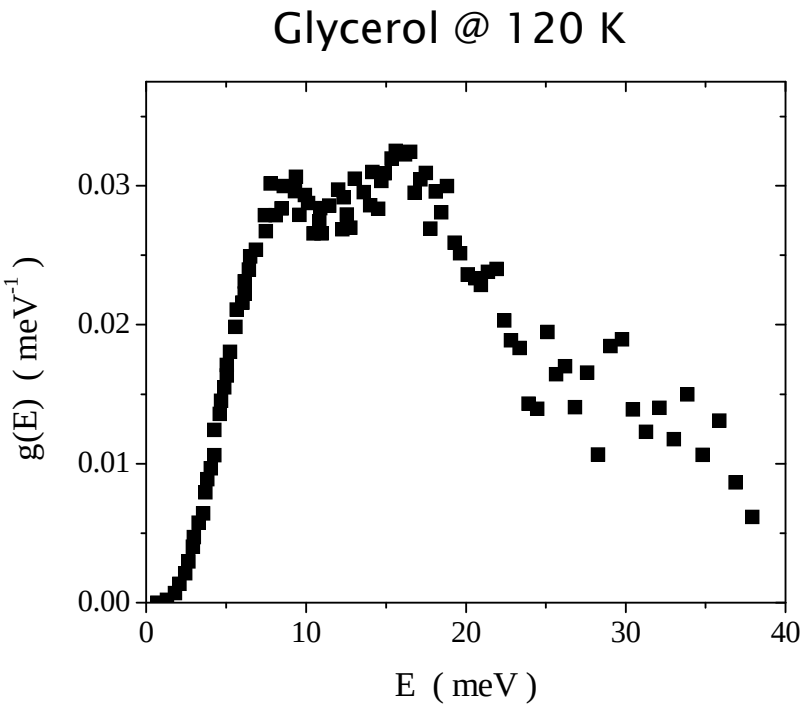

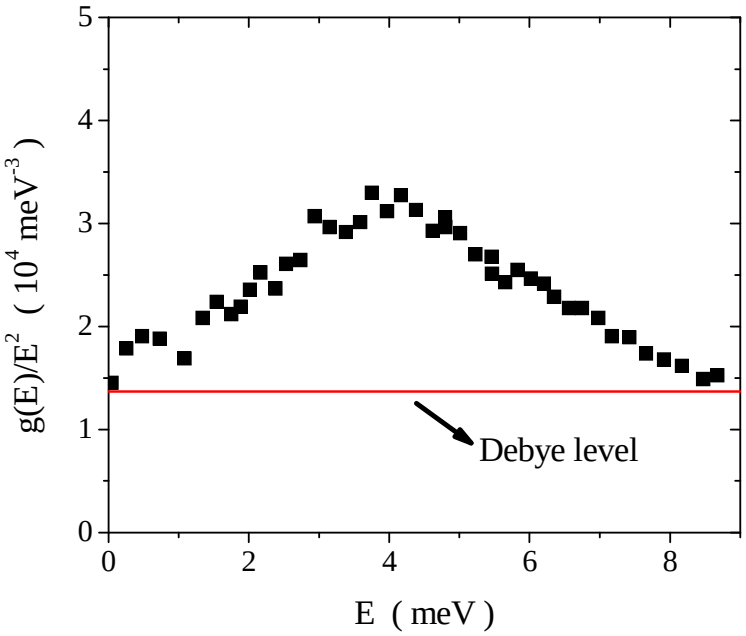

Wuttke et al., PRE 52, 4026 (95)

Excess in the density of states above the Debye level. What is the origin of these low-frequency modes?

The boson peak of glasses: models

• Defects in glasses can produce quasi-local, low-frequency states. These soft modes interact with the sound waves and hybridize with them, giving rise to the BP.

Parshin, Phys. Solid State 36, 991 (94); Gurevich et al., PRB 67, 094203 (03)

• Disorder in the force constants can smear and push to low frequency peaks which exist in the DOS of the corresponding crystal. Similar results in model systems with random spatial variations in the elastic moduli.

Schirmacher et al., PRL 81, 136 (91); Taraskin et al., PRL 86, 1255 (01)
Grigera et al., Nature 422, 289 (03)
Schirmacher, Europhys. Lett. 73, 892 (06)

• The BP marks the existence of nanometric inhomogeneities. Numerical studies show that the classical elasticity description breaks down in glasses on the mesoscopic length-scale.

Duval et al., JPCM 2, 10227 (90)
Leonforte et al., PRB 72, 224206 (05)

Experimental results

- Tunnel junction techniques: transverse modes show no dispersion up to 2 meV in SiO_2
- IXS: longitudinal acoustic-like branch unaffected across the boson peak position

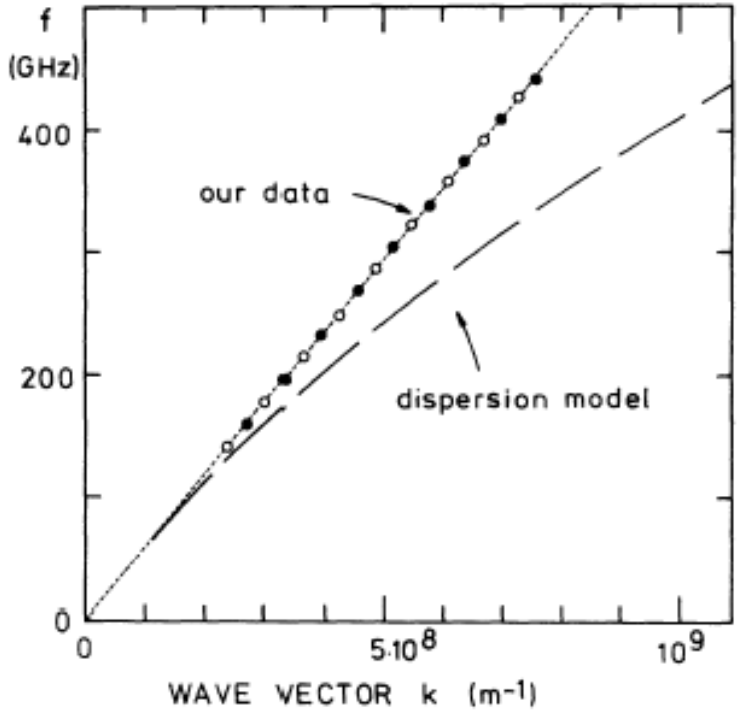

Rothenfusser et al., PRB 27, 5196 (83)

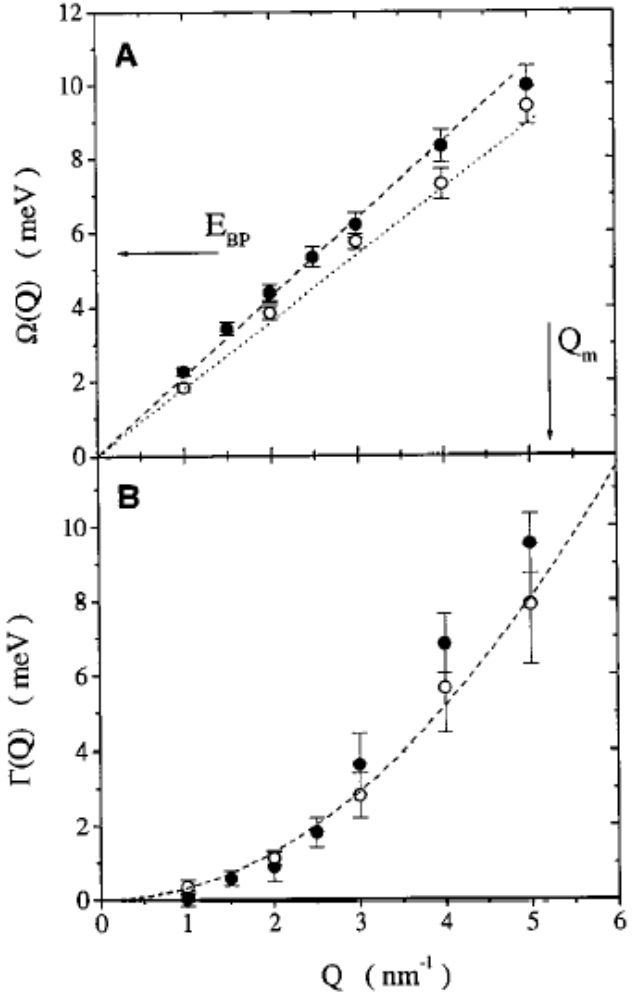

Sette et al., Science 280, 1550 (98)

The problem of the acoustic attenuation

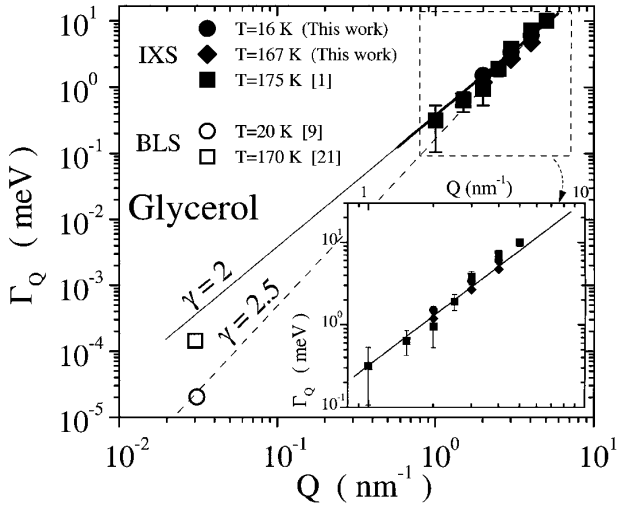

Ruocco et al., PRL 83, 5583 (99)

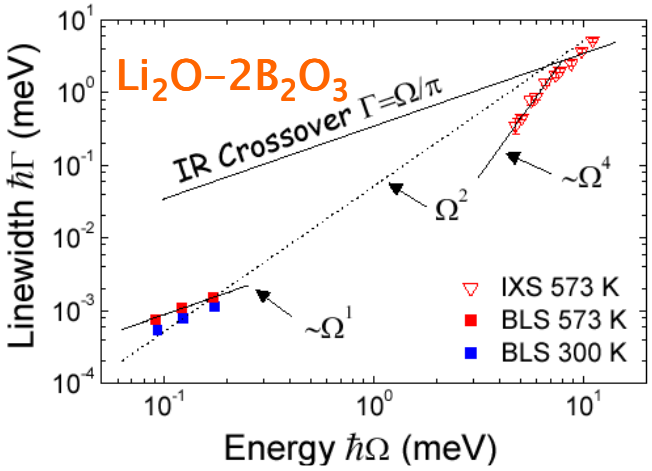

Rufflé et al., PRL 96, 045502 (06)

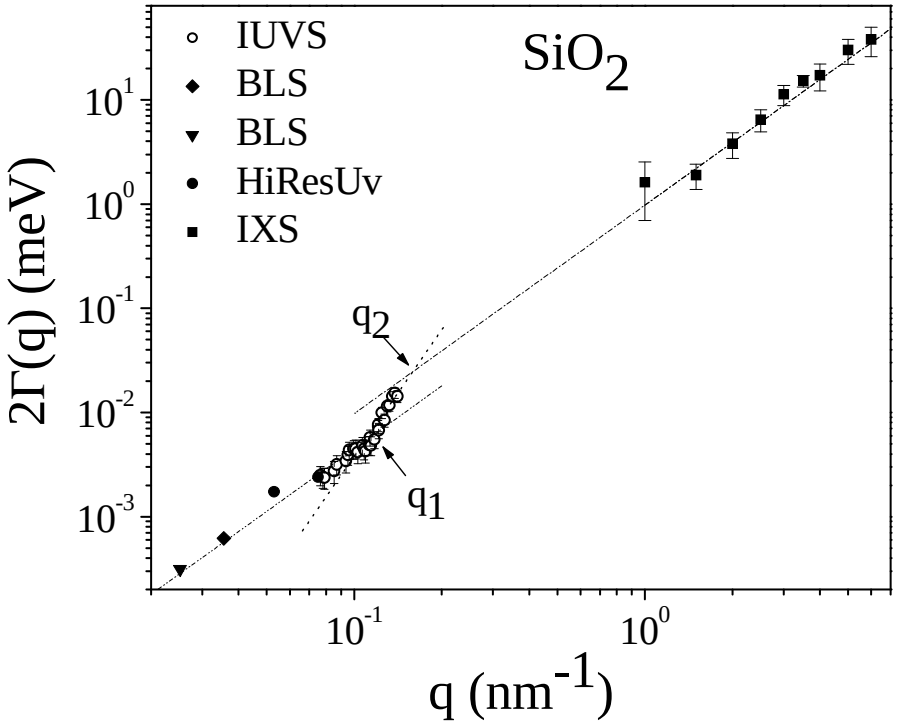

Masciovecchio et al., PRL 97, 035501 (06)

Is this phenomenology system-dependent ?

IXS: recent results

Glycerol @ 150 K

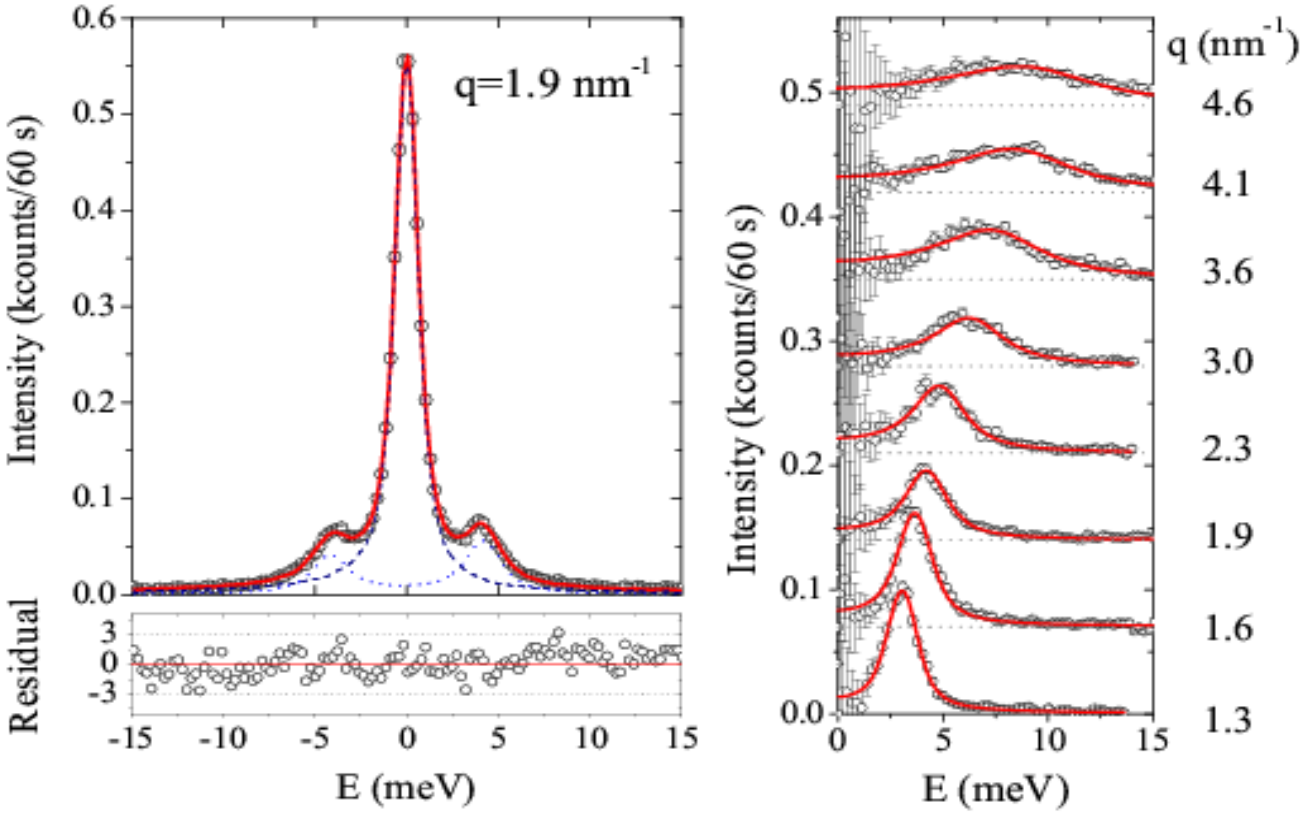

g.m. & Giordano, PNAS 106, 3659 (09)

Acoustic attenuation

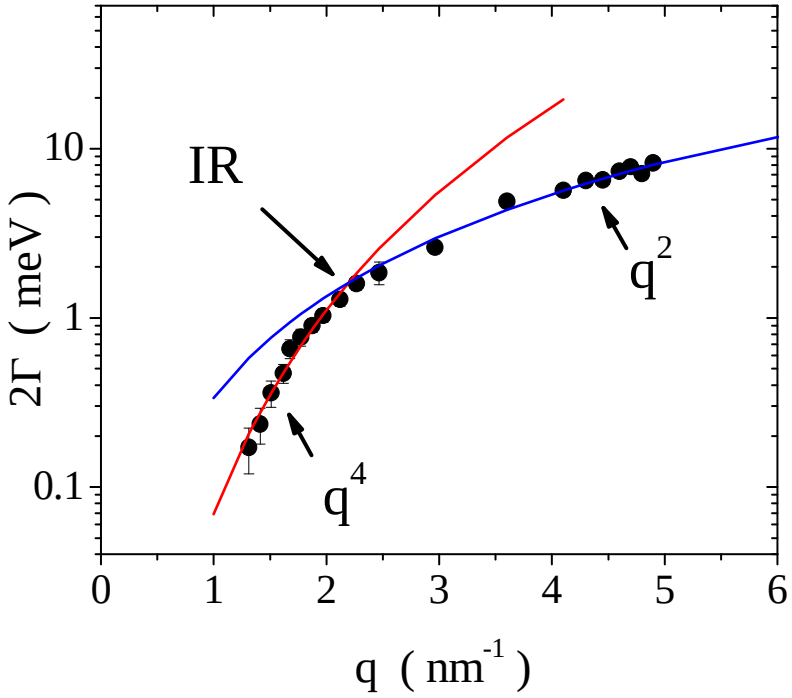

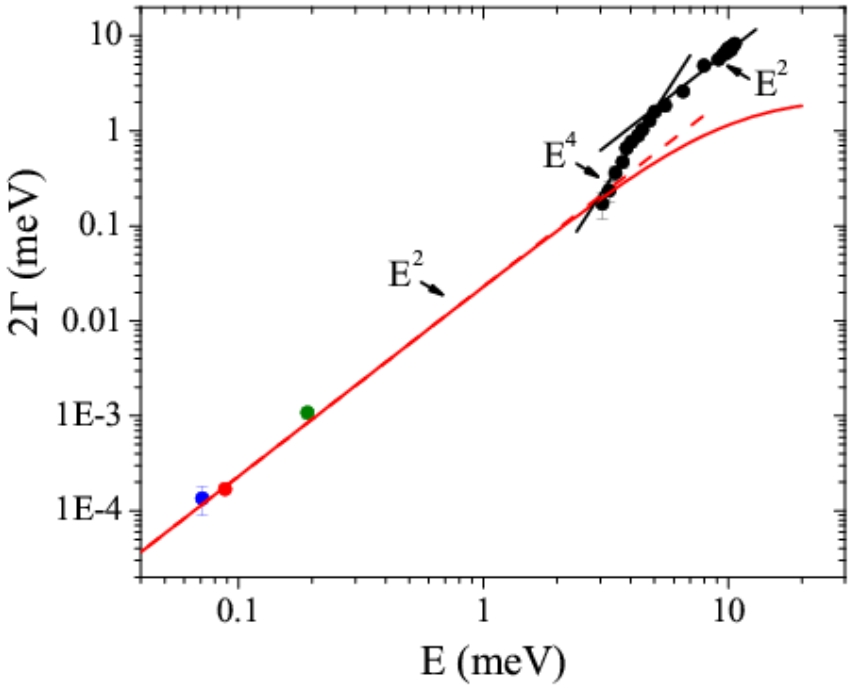

The q^4 to q^2 transition takes place close to the Ioffe-Regel limit defined as $\lambda_{IR}=2l$ ($\Omega/\pi=2\Gamma$)

anharmonic contribution:

$$2\,\Gamma = \frac{\gamma^2\, T\, C_v\, v_l\, \tau_{th}}{2\,\hbar\,\rho\, v_D^3}\, E^2$$

Dispersion curve

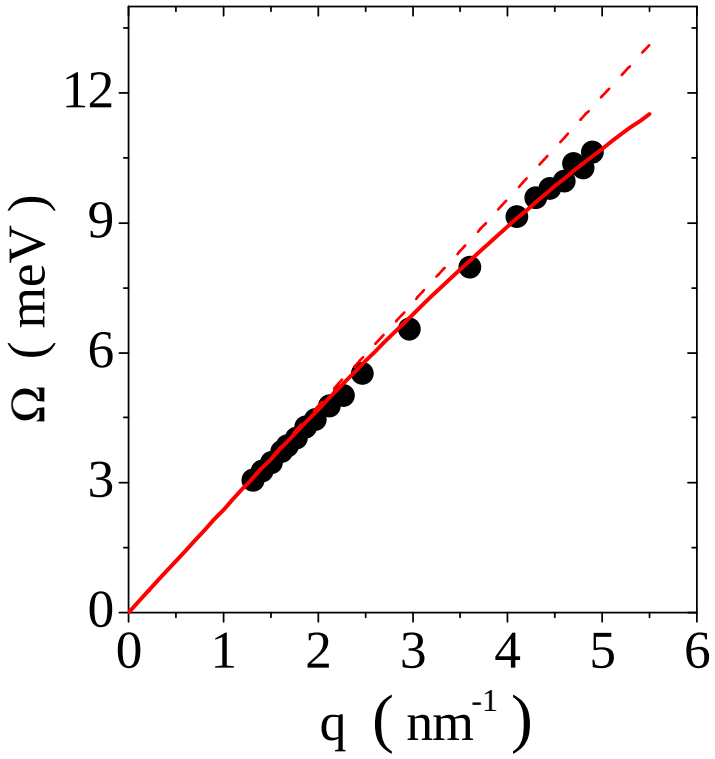

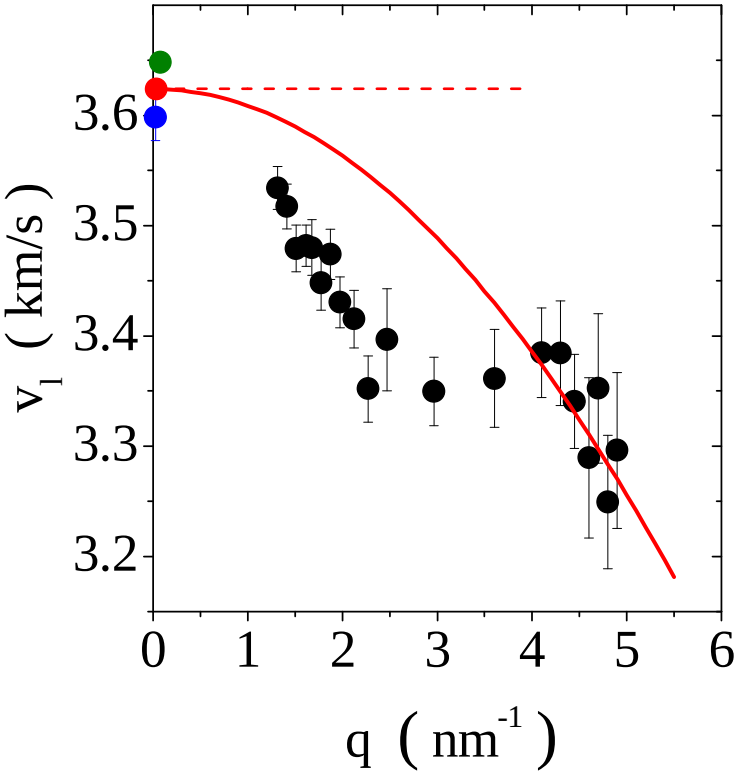

Low-frequency data from: Grubbs & MacPhail, JCP 100, 2561 (94);
Comez et al., JCP 119, 6032 (03); Masciovecchio et al., PRL 92, 247401 (04)

The boson peak

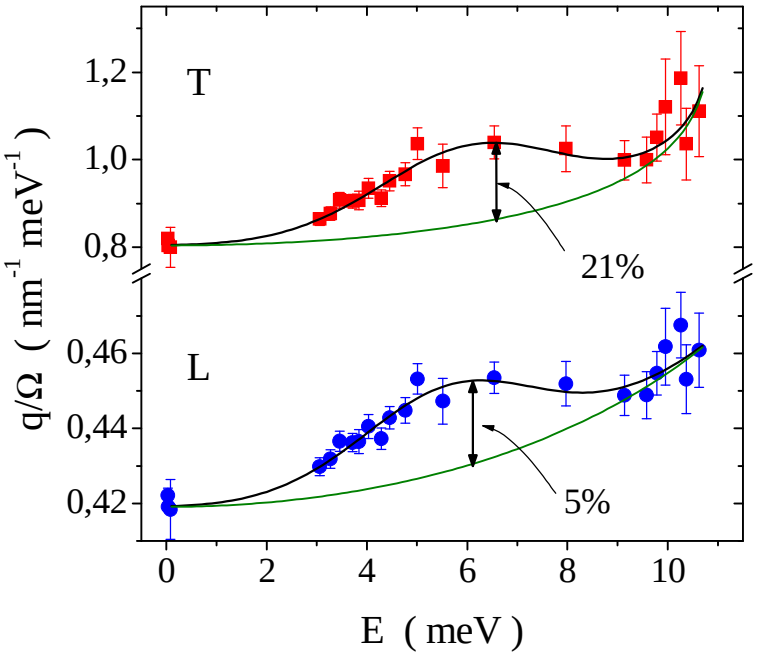

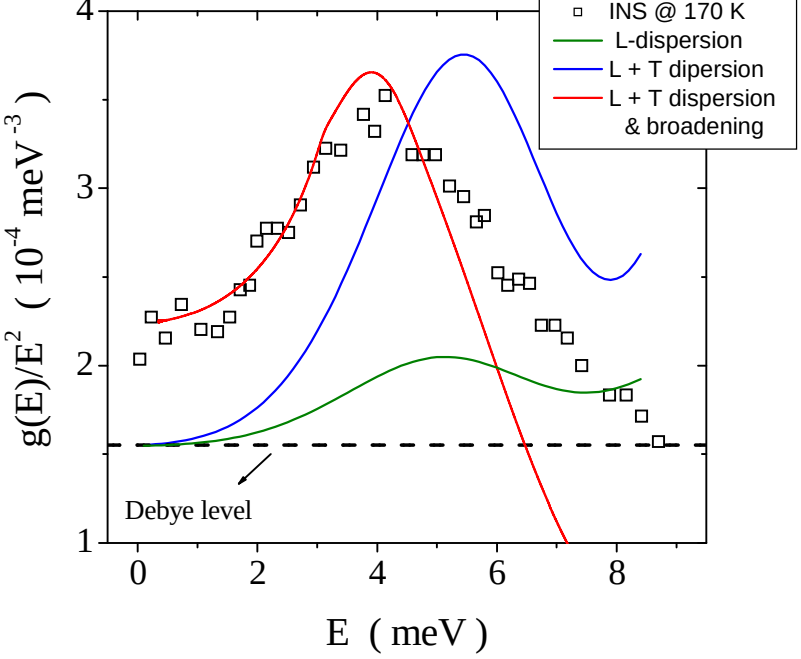

1. $$\frac{g(E)}{E^2} = \frac{1}{k_D^3}\left[\left(\frac{q^2}{E^2}\frac{\partial q}{\partial E}\right)_L + 2\left(\frac{q^2}{E^2}\frac{\partial q}{\partial E}\right)_T\right]$$

2. $$\frac{g(E)}{E^2} = \frac{1}{k_D^3}\int_0^{k_D} dq\left[\frac{S_L(q,E)}{v_0^2} + 2\,\frac{S_T(q,E)}{v_0^2}\right]$$

Conclusions - I

- The low-temperature universal anomalies of glasses are accompanied by anomalies in the elastic properties on the mesoscopic scale
- The acoustic branch in glasses shows a negative dispersion region in the energy range of the boson peak. At that point the Debye continuum approximation breaks down.
- This negative dispersion automatically provides to the glass "soft" modes with respect to the Debye expectation and, consequently, contributes (or gives rise) to the boson peak.
- The negative dispersion region is accompanied by an Ω^4 strong scattering regime which turns into an Ω^2 regime close to the Ioffe-Regel limit ($\Omega \sim \Gamma$).

Examples of experiments on liquids

Water anomalies: thermodynamics

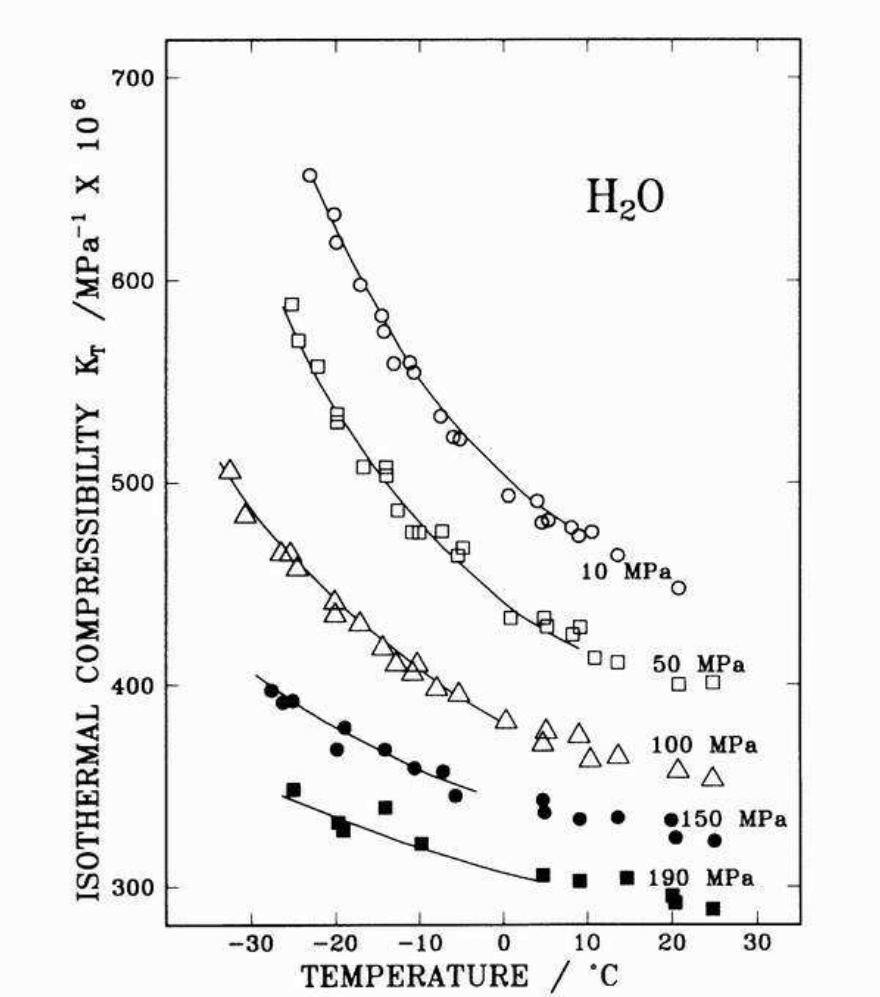

Kanno & Angell, J. Chem. Phys. 73, 1940 (1979)

$$K_T = -V^{-1}\left(\frac{\partial V}{\partial P}\right)_T$$

- Anomalous increase of compressibility upon cooling, with $K_T \sim (T-T_s)^{-\gamma}$
- Upon increasing pressure, the trends are similar, but the increases occur at progressively lower temperatures
- Being $S(0) = n K_B T K_T$, this also corresponds to an anomalous increase of density fluctuations.

Water anomalies: fast sound

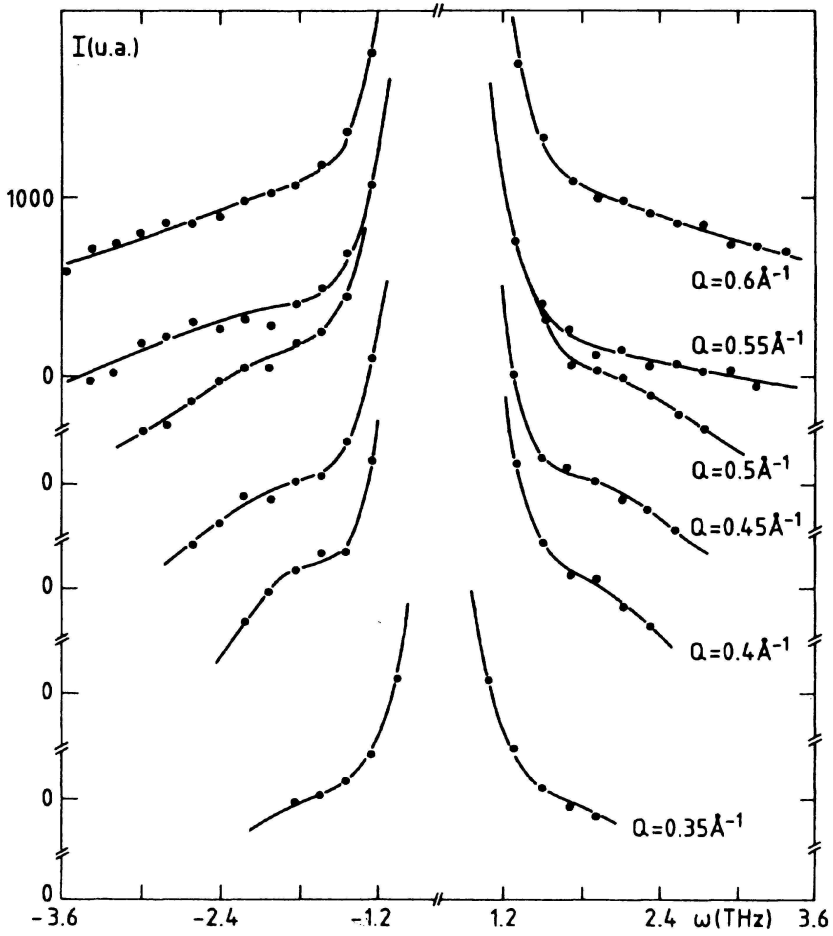

Teixeira et al., Phys. Rev. Lett. 54, 2681 (1985)

- Collective high-frequency sound mode observed by coherent inelastic neutron scattering.
- Mode interpreted as distinct from high-q limit of sound wave, rather being a collective excitation propagating in local hydrogen-bond structure.
- In a different study, it is concluded this mode comes from a rich variety of physical processes as reorientational relaxations and optical like modes of excitations.

Bermejo et al., Phys. Rev. E 51, 2250 (1995)

Inelastic x-ray scattering data on water

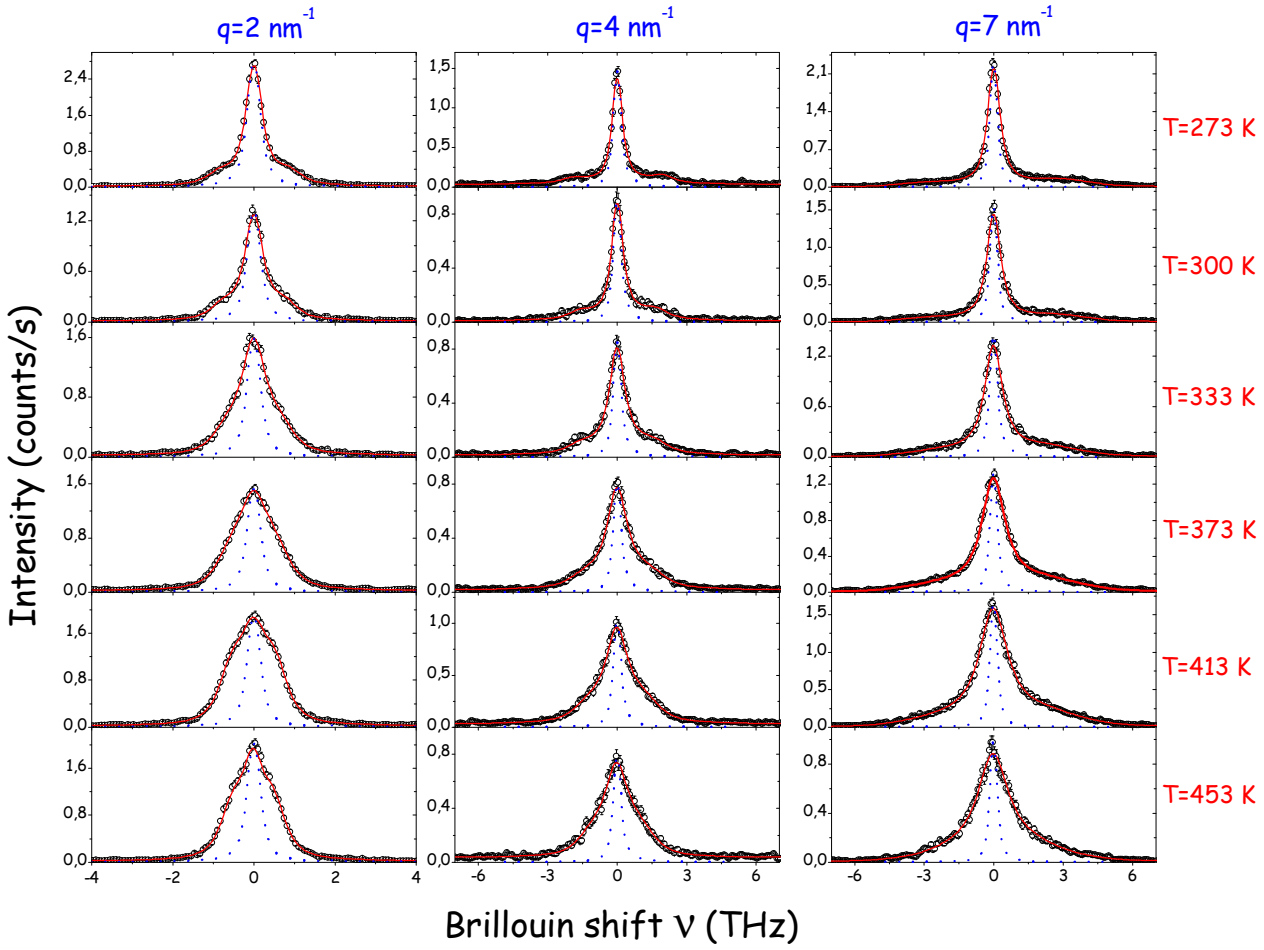

Models for the memory function - viscoelastic

(a) neglect q-dependence in the thermal parameters and in the isothermal compressibility since q << q_m

$$D_T(q) \rightarrow D_T$$
$$\gamma(q) \rightarrow \gamma$$
$$\omega_0(q) \rightarrow \omega_0 = c_T\, q$$

(b) two exponential approximation for $K_I(q,t)$ with one exponential " very fast ":

$$K_I(q,t) = 2\,\gamma_0(q)\,\delta(t) + q^2\,\Delta^2(q)\,\exp\left[-\frac{\omega_\infty^2(q)\,t}{\omega_0^2(q)\,\tau_C(q)}\right]$$

- $c_\infty(q)$ limiting sound speed
- $\gamma_o(q)$ q^2 times non-relaxing viscosity
- $\tau_c(q)$ compliance relaxation time

IXS experiments on water: viscoelastic analysis

Maxwell

τ_s [ps] ~ η_s / G_∞ ~ η_s [cP]

$$B + I_0\, R(\omega) \otimes [\,(n\,(\omega)+1)\cdot \cdot \mathrm{Im}[\omega^2 - \omega_0^2 + i\omega\, m_q\,(\omega)]^{-1}]$$

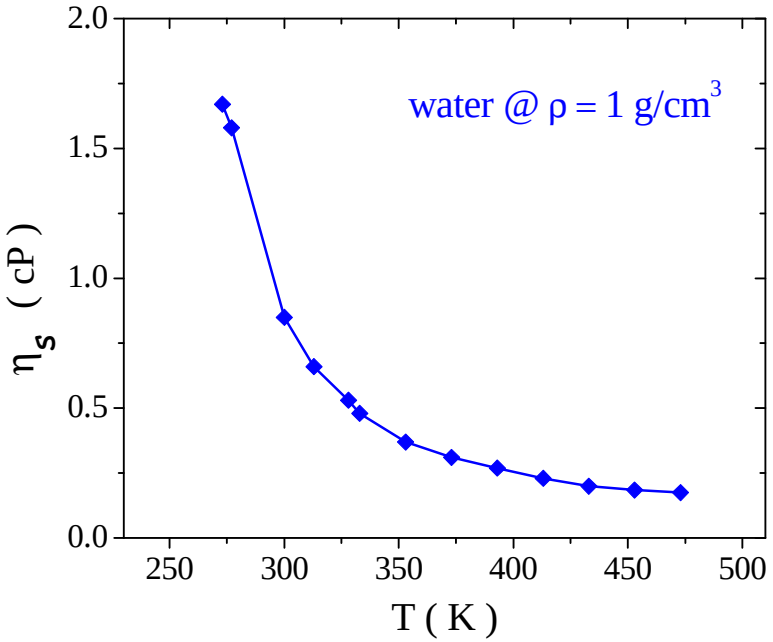

Kestin et al., J. Phys. Chem. Ref. Data 13, 175 (1984)

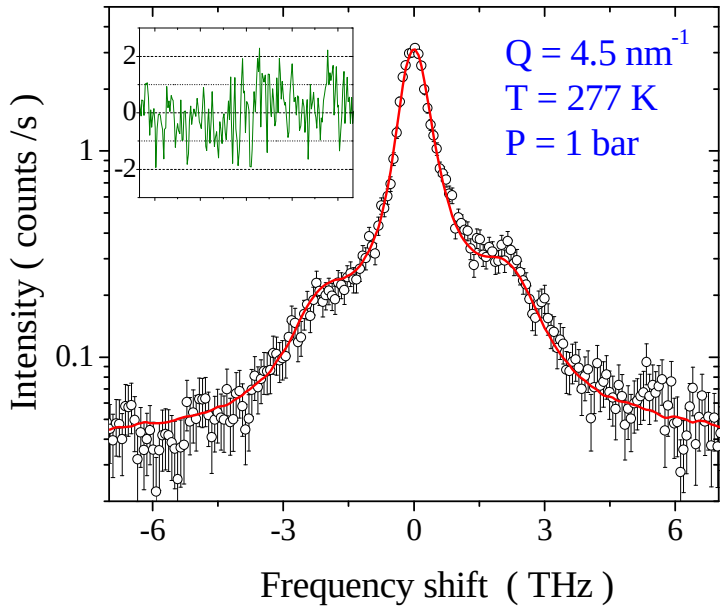

g.m. et al., Phys. Rev. E 60, 5505 (1999)

Liquid water – longitudinal viscosity

$$\Gamma(q) + q^2\Delta^2(q)\,\tau_M(q) \xrightarrow[q\to 0]{} q^2 \nu_l(q)$$

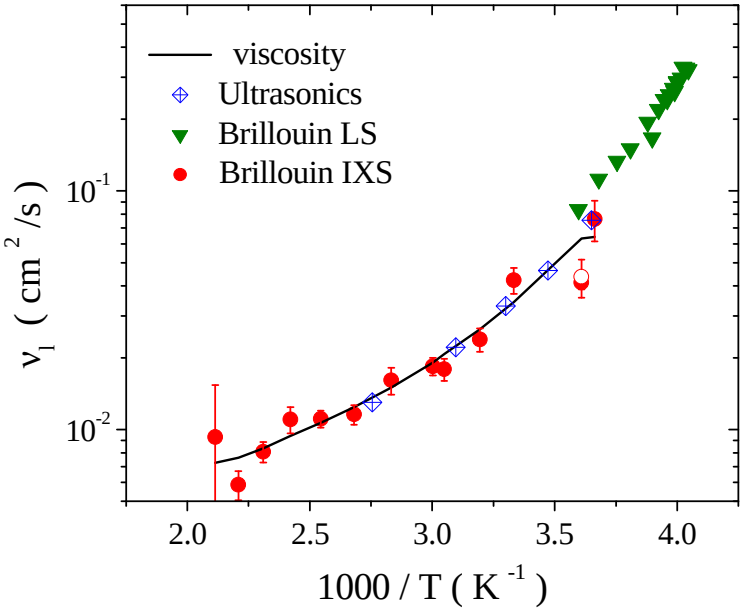

- The low-q limit of the fitting parameters correctly reproduces the longitudinal viscosity.

- The ratio between longitudinal and shear viscosity appears to be constant in all of the explored conditions – a fact which seems a prerogative of many H-bonded liquids.

- The overall shape of ν_l shows a temperature dependence stronger than the Arrhenius one.

Liquid water – fast sound

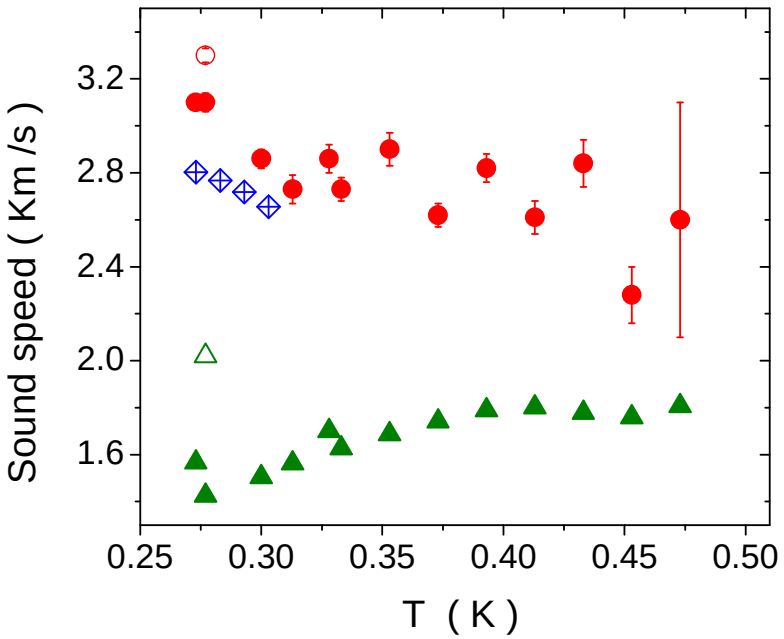

- IXS (Viscoelastic model) [Monaco et al., 1999]
- US @ 25 MHz [Slie et al., 1966]
- Thermodynamics [Kestin et al., 1984]

- The limiting speed of water is confirmed to be ~ 3000 m/s.
- The values of c_∞ and of Δ^2 both decrease with increasing temperature.
- Positive comparison with the ultrasound results obtained extrapolating ultrasonic measurements in water-glycerol mixtures towards the pure water limit.

Liquid water – relaxation time

In the thermodynamic range spanned by IXS τ shows an Arrhenius behaviour with activation energy $E_a = (3.8 \pm 0.6)$ kcal mol^{-1}

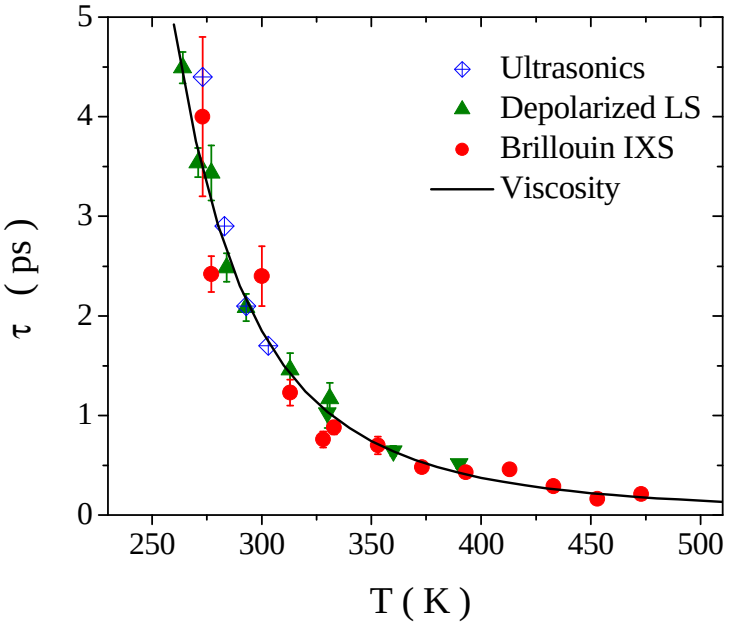

g.m. et al., Phys. Rev. E 60, 5505 (1999)

Macroscopic viscoelasticity is recovered below q~2 nm^{-1}

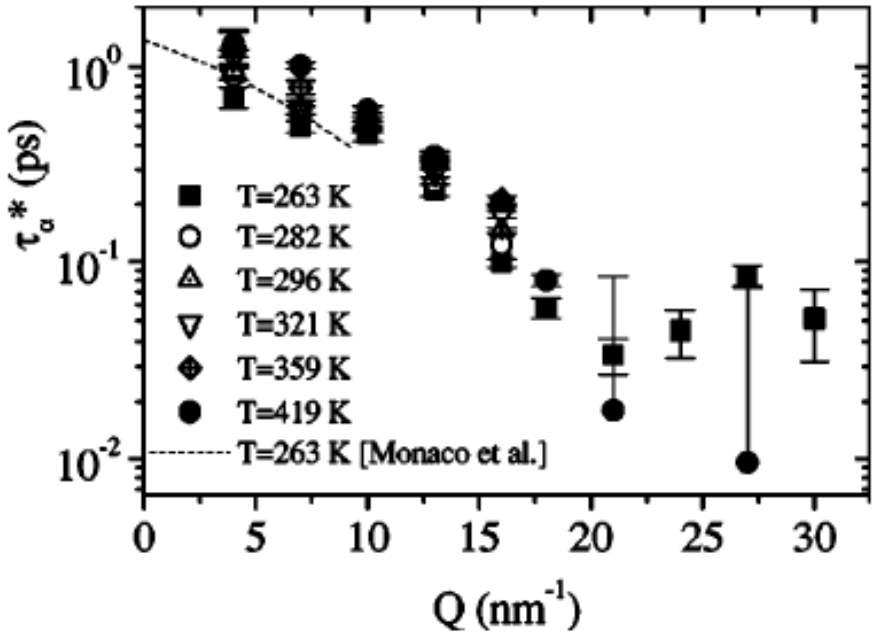

Pontecorvo et al., Phys. Rev. E 71, 011501 (2005)

Conclusions - II

• For $q \leq 2$ nm^{-1}, a hydrodynamic formalism with a frequency-dependent but q-independent memory function can be consistently used. The obtained results favorably compare with those of lower frequency techniques.

• For $q > 2$ nm^{-1}, a q-dependent memory function has necessarily to be introduced. Thus, the atomic dynamics in water has a homogeneous character down to a length-scale of ≈ 3 nm.

• The acoustic dynamics of water in the studied temperature and pressure range shows no anomalies. The positive dispersion and the relaxational effects on the acoustic excitations are very similar to what is found in other studied liquids.